

# Remarkable Predictive Power of the Modified Long Wavelength Approximation

Ilya L. Rasskazov,<sup>†</sup> Vadim I. Zakomirnyi,<sup>\*,‡,¶</sup> Anton D. Utyushev,<sup>‡,¶</sup> P. Scott  
Carney,<sup>†</sup> and Alexander Moroz<sup>\*,§</sup>

<sup>†</sup>*The Institute of Optics, University of Rochester, Rochester, NY 14627, USA*

<sup>‡</sup>*Siberian Federal University, Krasnoyarsk, 660041, Russia*

<sup>¶</sup>*Institute of Computational Modelling of the Siberian Branch of the Russian Academy of  
Sciences, Krasnoyarsk, 660036, Russia*

<sup>§</sup>*Wave-scattering.com*

E-mail: vadimza@icm.krasn.ru; wavescattering@yahoo.com

## Abstract

The modified long-wavelength approximation (MLWA), a next order approximation beyond the Rayleigh limit, has been applied usually only to the dipole  $\ell = 1$  contribution and for the range of size parameters  $x$  not exceeding  $x \lesssim 1$  to estimate far- and near-field electromagnetic properties of plasmonic nanoparticles. Provided that the MLWA functional form for the  $T$ -matrix elements in a given channel  $\ell$  is limited to the ratio  $T \sim iR/(F + D - iR)$ , where  $F$  is the familiar size-independent Fröhlich term, with  $\varepsilon$  being dielectric constant, and  $R \sim \mathcal{O}(x^{2\ell+1})$  is a radiative reaction term, there is a one-parameter freedom in selecting the dynamic depolarization term  $D \sim \mathcal{O}(x^2)$  which preserves the fundamental feature of the MLWA that its predictions coincide with those of the Mie theory up to the order  $\mathcal{O}(x^2)$ . By exploiting this untapped design freedom, we demonstrate on a number of different metals (Ag, Al, Au, Mg),

and using real material data, that the MLWA may surprisingly yield very accurate results for plasmonic spheres both for (i)  $x$  up to  $\gtrsim 1$  and beyond, and (ii) higher order multipoles ( $\ell > 1$ ), essentially doubling its expected range of validity. Because the MLWA obviates the need of using spherical Bessel and Hankel functions and allows for an intuitive description of (nano)particle properties in terms of a driven damped harmonic oscillator parameters, a significantly improved analysis and understanding of nanoparticle scattering and near-field properties can be achieved.

## Introduction

For over one century, the Mie theory,<sup>1</sup> which provides a rigorous and complete description of the light scattering from spherical particles, has been indispensable tool for numerous applications. The theory offers a reliable description of electromagnetic fields inside, in a close proximity of, or far away from spherical particles of any material, and has been employed in ongoing development of plasmonic applications of small metal particles in biology, energy conversion, medicine, sensing, and many other fields. Nonetheless, the Mie theory did not prevent continuous attempts in intuitive understanding of the light scattering in more simple terms, which would offer a deeper physical insight into the nature of light-matter interactions. Just on contrary, nowadays the popularity of alternative intuitive description of light scattering appears to be greater than ever before, as witnessed by applications of coupled mode theory,<sup>2-4</sup> coupled harmonic oscillators model,<sup>5-7</sup> and modal expansions.<sup>8-10</sup> The prime example is the *Rayleigh limit*, which preceded the Mie theory<sup>1</sup> and, in spite of its obvious numerous deficiencies (e.g. cannot account for a size dependent red-shift of the localized surface plasmon resonance (LSPR) (cf. sec 12.1.1. of ref 11) and predicts zero extinction and negative absorption for purely dielectric particles), it has been repeatedly used in various analytic considerations to describe LSPR, the basics of surface-enhanced Raman spectroscopy (SERS)<sup>12</sup> and other plasmonic properties.

The focus of the present work is on the so-called modified long-wavelength approximation

(MLWA),<sup>13-23</sup> which is a next order approximation beyond the Rayleigh limit. The present study is limited to spherical particles, in which case the MLWA yields results coinciding with the Mie theory up to the order  $\mathcal{O}(x^2)$ , with  $x = kr_s$  being the conventional size parameter, where  $r_s$  is spherical particle radius and  $k$  is wave vector of an incident plane wave in the host medium. The MLWA overcomes the main shortcoming of the quasi-static Rayleigh limit and has been known to rather precisely capture *size-dependence* of the elementary cross sections, including the red-shift of the LSPR (sec 12.1.1. of ref 11), an additional red-shift of the near-field intensity peak relative to the LSPR,<sup>22</sup> and local field enhancements. Usually, like the Rayleigh limit, the MLWA was, with a notable exception,<sup>21</sup> applied only to the electric dipole ( $\ell = 1$ ) contribution. The results of refs 21,23 have shown that the MLWA can be surprisingly accurate not only for  $x \lesssim 1$  (which is the expected range of validity of the MLWA by its very definition), but also for higher order multipole contributions ( $\ell > 1$ ), and for  $x$  well above unity.<sup>21,23</sup> The unexpected accuracy of the MLWA is a pleasant and very useful surprise that deserves further examination.

Schebarchov et al.<sup>21</sup> needed to keep terms up to the order  $\mathcal{O}(x^4)$  in the expansion of spherical Bessel functions to achieve reliable results for  $x \gtrsim 1$ . Surprisingly enough, we show here that one can improve on the predictive power of the  $\mathcal{O}(x^4)$  approximation of ref 21 by keeping only terms  $\mathcal{O}(x^2)$  upon optimizing the so-called *dynamic depolarization* term. Our focus on the  $\mathcal{O}(x^2)$ -MLWA is that, at least in the dipole case, only the  $\mathcal{O}(x^2)$ -MLWA allows for an intuitive description of scattering and near-field properties of Drude-like plasmonic particles in terms of a driven damped harmonic oscillator with the Abraham-Lorenz force, mass, and stiffness directly related to corresponding partial depolarization terms.<sup>22</sup> Such an intuitive description is easy to analyze, which may result in a significantly improved understanding of nanoparticle scattering and its near-field, thereby facilitating design of (nano)particles with desired properties. Our optimized  $\mathcal{O}(x^2)$ -MLWA captures photonic properties of a particle as an interplay of three basic terms: a quasi-static *Fröhlich* term  $F$ , the dynamic depolarization term  $D$  ( $\sim x^2$ ), and a *radiative reaction* term  $R$  ( $\sim x^{2\ell+1}$ ),

while providing better match to the Mie theory than that obtained in earlier works.<sup>21,23</sup> We demonstrate this in detail for various plasmonic particles (Ag, Al, Au, Mg) for  $\ell \geq 1$  and beyond  $x = 1$  on using real material data.<sup>24,25</sup> The optimized MLWA will be shown to yield remarkable agreement of the peak position and height with those in the exact Mie theory, and to possess an enlarged range of validity essentially twice as large as it has been initially expected.

Particle electric multipole polarizabilities  $\alpha_\ell$  can be obtained in the quasi-static limit from the corresponding  $T$ -matrix elements  $T_{E\ell}$  conveniently described by MLWA. Therefore, any quasi-static method intrinsically based on elementary polarizabilities, such as Maxwell-Garnett homogenization formulas,<sup>26-28</sup> a coupled-dipole (CDA) or discrete-dipole approximation (DDA),<sup>29-31</sup> Gersten and Nitzan approximation for determining nonradiative decay rates<sup>32,33</sup> can, in principle, be immediately improved by adopting our results. An insight provided by our MLWA can be also straightforwardly employed in layer and bulk Korringa-Kohn-Rostocker photonic multiple-scattering theories<sup>34-38</sup> to analyze in simple terms the effect of periodic arrangement of spherical scatterers in a plane, or in a three-dimensional lattice, on various single-sphere multipole contributions.

## Notation, Definitions, and the Rayleigh Limit

The resulting cross sections for a plane electromagnetic wave scattering from a spherical particle of radius  $r_s$  are given as an infinite sum over all momentum channels  $\ell \geq 1$  and both polarizations.<sup>11,39</sup> According to eqs 2.135-8 of ref 39, any given angular momentum channel  $\ell$  and polarization  $p$  ( $p = E$  for electric (or TM) polarization, and  $p = M$  for magnetic (or TE) polarization) contributes the following partial amount to the resulting scattering, absorption, and extinction cross sections,

$$\sigma_{sca;p\ell} = \frac{2(2\ell + 1)\pi}{k^2} |T_{p\ell}|^2, \quad (1)$$

$$\sigma_{abs;p\ell} = -\frac{2(2\ell + 1)\pi}{k^2} [|T_{p\ell}|^2 + \Re(T_{p\ell})], \quad (2)$$

$$\sigma_{ext;p\ell} = -\frac{2(2\ell + 1)\pi}{k^2} \Re(T_{p\ell}), \quad (3)$$

where  $k = 2\pi/\lambda$  is the wavenumber, with  $\lambda$  being the incident wavelength in the *host medium*. In an optical convention,  $-T_{p\ell}$  are nothing but familiar Mie's expansion coefficients  $a_\ell$  and  $b_\ell$  (eqs 4.53 of ref 11), i.e.  $T_{E\ell} = -a_\ell$  and  $T_{M\ell} = -b_\ell$ . The resulting full cross sections are determined as an infinite sum

$$\sigma_{sca} = \sum_{p,\ell} \sigma_{sca;p\ell}, \quad \sigma_{abs} = \sum_{p,\ell} \sigma_{abs;p\ell}, \quad \sigma_{ext} = \sum_{p,\ell} \sigma_{ext;p\ell}.$$

In the case of a homogeneous sphere, Mie solution<sup>1</sup> explicitly determines the respective  $T$ -matrix elements in a given  $\ell$ th angular momentum channel as (eqs 2.127 of ref 39)

$$T_{p\ell} = -\frac{v[xj_\ell(x)]'j_\ell(x_s) - j_\ell(x)[x_sj_\ell(x_s)]'}{v[xh_\ell(x)]'j_\ell(x_s) - h_\ell(x)[x_sj_\ell(x_s)]'}, \quad (4)$$

where the respective  $j_\ell$  and  $h_\ell = h_\ell^{(1)}$  are the conventional spherical Bessel and Hankel functions (sec 10 of ref 40), prime denotes the derivative with respect to the argument,  $x = kr_s$  is the conventional dimensionless size parameter,  $x_s = xn$ , where  $n = n_s/n_h = \sqrt{\varepsilon_s\mu_s/(\varepsilon_h\mu_h)}$  is the relative refractive index contrast of the sphere ( $n_s$ ) and the host ( $n_h$ ), and  $\varepsilon_s$  ( $\varepsilon_h$ ) is the sphere (host) permittivity, and  $\mu_s$  ( $\mu_h$ ) is the sphere (host) permeability. One has, assuming nonmagnetic media,  $v = \mu_s/\mu_h = 1$  for magnetic polarization, and  $v = \varepsilon := \varepsilon_s/\varepsilon_h$  for electric polarization.

In the familiar Rayleigh limit,

$$T_{E1} \rightarrow T_{E1;R} = \frac{2ix^3}{3} \frac{\varepsilon - 1}{\varepsilon + 2} \quad (x \ll 1). \quad (5)$$

The overall  $x^3$ -factor of  $T_{E1;R}$  in eq 5 affects only the magnitude of  $T_{E1;R}$ , but not its structure (i.e. a peak position). Because  $T_{E1;R}$  is *purely imaginary* for real  $\varepsilon_s$ , the resulting extinction cross section  $\sigma_{ext;E1}$  for purely dielectric sphere is, in virtue of  $\Re(T_{E1;R}) = 0$  in eq 3, identically zero in the Rayleigh limit. Hence  $\sigma_{ext;E1} \neq \sigma_{sca;E1} + \sigma_{abs;E1}$ , which violates unitarity.<sup>41</sup> Even worse, the resulting absorption cross section  $\sigma_{abs;E1}$  for purely dielectric, and hence nonabsorbing, sphere is, in virtue of  $\Re(T_{E1;R}) = 0$  in eq 2, *negative*,  $\sigma_{abs;E1} = -\sigma_{sca;E1} < 0$ . The modulus of  $T_{E1;R}$  is also not prevented from exceeding unity, implying complex phase shifts for  $\varepsilon \approx -2$ . From the above fundamental perspective, the Rayleigh limit fails miserably and it is a wonder that the Rayleigh limit is used so often and in so many different settings.<sup>12,42,43</sup>

## Taming the Zoo of MLWA's

The usual MLWA<sup>13,15,17,20,21</sup> is a limiting form of the Mie dipole term for  $x \lesssim 1$ , that, unlike the quasi-static Rayleigh approximation (eq 5), keeps both dynamic depolarization ( $D \sim x^2$ ) and radiative reaction ( $R \sim x^3$ ) terms. The MLWA for a general  $\ell$  and  $p$  is required to reproduce the Mie theory results up to the order  $\mathcal{O}(x^2)$ . It combines in a concise way three different elementary terms, involving the dynamic depolarization ( $D \sim x^2$ ) and radiative reaction ( $R \sim x^{2\ell+1}$  for  $p = E$  and  $R \sim x^{2\ell+3}$  for  $p = M$ ), in the functional form

$$T_{p\ell} \sim \frac{iR(x)}{F + D(x) - iR(x)}, \quad (6)$$

where

$$F := v + \frac{\ell + 1}{\ell} \quad (7)$$

is a *size-independent* quasi-static Fröhlich term. Without going yet in to the details of  $D$  and  $R$ , the sole functional form (eq 6) makes it already transparent that the usual Rayleigh limit (eq 5), which amounts to setting  $D(x) = R(x) \equiv 0$  in the denominator, is essentially

recovered for  $x, x_s \ll 1$ ,  $\ell = 1$ , and  $p = E$ . The vanishing of the size-independent  $F$  in the denominator yields the usual quasi-static Fröhlich LSPR condition, which determines the quasi-static LSPR frequencies  $\omega_{0\ell}$ . In the case of Drude fit of  $\varepsilon_s$ ,

$$\varepsilon_s = \varepsilon_\infty - \frac{\omega_p^2}{\omega(\omega + i\gamma)},$$

where  $\varepsilon_\infty$  is the high-frequency permittivity limit,  $\omega_p$  is the bulk plasma frequency, and  $\gamma$  is a damping constant, one finds  $\omega_{0\ell} = \omega_p / \sqrt{\varepsilon_\infty + [(\ell + 1)\varepsilon_h / \ell]}$ . A size-dependent red shift of the dipole LSPR, which cannot be accounted for by the Rayleigh approximation, is determined by solving for the zeros of the sum  $F + D(x) = 0$ . For purely *real*  $v$  all the terms  $F, D, R$  are real. Although the order of  $R$  of at least  $\sim x^{2\ell+1}$  in the denominator is larger than that of  $x^2$ , it is its presence there which ensures for purely real  $v$  that  $|T_{p\ell}|^2 = -\Re(T_{p\ell})$ , i.e.  $\sigma_{abs;\ell} \equiv 0$  (cf. eq 2), and unitarity  $\sigma_{ext;\ell} = \sigma_{sca;\ell}$  (cf. eqs 1, 3). Furthermore, keeping  $R(x)$  in the denominator prevents the modulus of  $T_{p\ell}$  from exceeding unity for  $x \gtrsim 1$ .

The restriction  $\sigma_{abs;\ell} \geq 0$  translates on substituting eq 6 into eq 2 in the constraint

$$\Im \{R(x)[F^* + D^*(x)]\} \geq 0. \quad (8)$$

Rigorously speaking, provided that we perform the limit  $x, x_s \ll 1$  in each of the numerator and denominator of the  $T$ -matrix (eq 4) following the recipe that

**(R1)** only terms up to  $\mathcal{O}(x^2)$  order in the asymptotic expansion of each spherical Bessel function in eq 4 are kept (see chapter 10 of ref 44)

**(R2)** in a product of a spherical Bessel and Hankel functions, or of two Bessel functions, again only terms up to  $\mathcal{O}(x^2)$  order are kept and all higher order terms are neglected

any such a limit functional form (eq 6) is *ambiguous* (see the Supporting Information). For example, one can arrive in a given  $(E\ell)$  channel for nonmagnetic media characterized by

$\varepsilon = n^2$  at (see the Supporting Information)

$$T_{E\ell} \sim \frac{iR_{E\ell}(x) \left[1 + \frac{\varepsilon x^2}{(\ell+1)(2\ell+3)}\right]}{F + \frac{\varepsilon}{(\ell+1)(2\ell+3)} \left[\varepsilon - \frac{(\ell+1)(2\ell+3)}{\ell(2\ell-1)}\right] x^2 - iR_{E\ell}(x)} \quad (9)$$

$$\sim \frac{iR_{E\ell}(x)}{F - \frac{2(2\ell+1)}{\ell(2\ell-1)(2\ell+3)} \varepsilon x^2 - iR_{E\ell}(x)} \quad (10)$$

$$\sim \frac{iR_{E\ell}(x) \left[1 - (\varepsilon + 1) \frac{x^2}{2(2\ell+3)}\right]}{F + \left[-\varepsilon^2 - \frac{3(2\ell+1)}{\ell(2\ell-1)} \varepsilon + \frac{(\ell+1)(2\ell+3)}{\ell(2\ell-1)}\right] \frac{x^2}{2(2\ell+3)} - iR_{E\ell}(x)} \quad (11)$$

$$\sim \frac{iR_{E\ell}(x)}{F + \left(\frac{\ell-2}{\ell+1} \varepsilon + 1\right) \frac{(\ell+1)(2\ell+1)}{\ell(2\ell-1)(2\ell+3)} x^2 - iR_{E\ell}(x)}, \quad (12)$$

where

$$R_{E\ell}(x) := \frac{(\varepsilon - 1)(\ell + 1)x^{2\ell+1}}{\ell(2\ell - 1)!!(2\ell + 1)!!}. \quad (13)$$

All the above eqs 9–12 constitute legitimate MLWA's. The expression 9 results from (i) first factorizing the  $T$ -matrix in terms of the so-called  $K$ -matrix and (ii) taking the limit  $x, x_s \ll 1$  in the  $K$ -matrix (see the Supporting Information). The expression 11 results from taking the limit  $x, x_s \ll 1$  directly in the numerator and denominator of the  $T$ -matrix in eq 4. Provided that the numerator of the  $T$ -matrix has the form  $R_{E\ell}[1 + Ax^2]$  as in eqs 9, 11, following our recipe **(R1)**-**(R2)** we can either ignore the  $\mathcal{O}(x^2)$  term in the square bracket in therein, or we may decide to multiply the numerator and denominator of any of the above expression (eqs 9, 11) by  $f = 1 - Ax^2$ . The latter provision will transform the  $\mathcal{O}(x^2)$  term in the numerator into  $\mathcal{O}(x^4)$  term, which is subsequently ignored. However, this provision brings about a change of  $D$  in the denominator. This way one arrives at further alternative MLWA expressions. For example, eq 10 is obtained from eq 9 by multiplying both the numerator and denominator of the rhs of eq 9 by  $1 - \varepsilon x^2/[(\ell + 1)(2\ell + 3)]$ .  $D(x)$  in eq 12 is obtained from eq 11 by multiplying both the numerator and denominator of the latter by  $1 + (\varepsilon + 1)x^2/[2(2\ell + 3)]$ . All expressions 9–12 make it transparent that  $T_{E\ell}$  in any given channel is determined solely by a size-independent quasi-static Fröhlich term  $F$  (eq 7), a



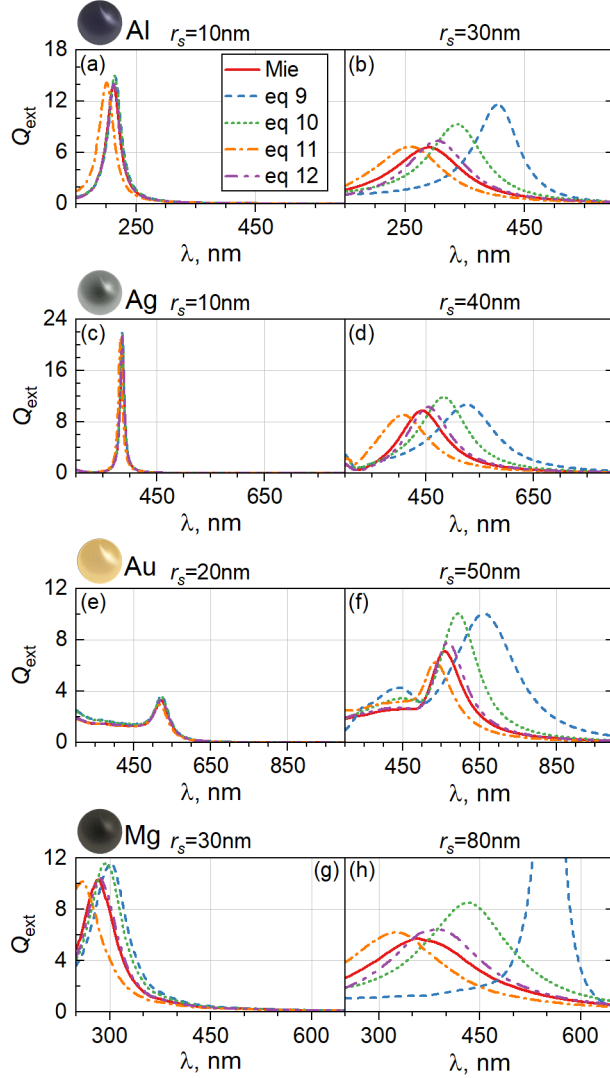


Figure 1: Comparison of extinction spectra for (a), (b) Al, (c), (d) Ag, (e), (f) Au, (g), (h) Mg NPs with different radii  $r_s$  in water ( $n_h = 1.33$ ) host as calculated for electric dipole, ( $E1$ ) channel, via exact Mie theory, eq 4, and via different limiting expressions for MLWA: eqs 9–12. Notice almost the same accuracy of MLWA’s for small  $r_s$  (left), and different accuracy for large  $r_s$  (right). Real material data is used for Al, Ag, Au<sup>24</sup> and Mg.<sup>25</sup>

*dynamic depolarization* term  $D$  ( $\sim x^2$ ), and a *radiative reaction* term  $R_{E\ell}$  (eq 13). However, as illustrated in Figure 1, MLWA's predictions may dramatically differ for  $x, x_s \gtrsim 1$ , in spite of that they all agree for  $x, x_s \ll 1$ . As obvious from Figure 1, the MLWA of eq 12 stands out by its performance from  $x \ll 1$  up to  $x \gtrsim 1$ .<sup>21,23</sup> Nevertheless, all MLWA's correctly account up to  $\mathcal{O}(x^2)$ -term for a size-dependent red shift of the dipole LSPR, whereas the Rayleigh approximation does not. For instance, for  $\ell = 1$ , eq 12 becomes (cf. eq A3 of ref 17)

$$T_{E1} \sim \frac{2ix^3}{3} \frac{(\varepsilon - 1)}{\varepsilon + 2 - \frac{3}{5}(\varepsilon - 2)x^2 - \frac{2i}{3}(\varepsilon - 1)x^3}. \quad (14)$$

On substituting into eqs 1–3, one finds the following cross sections of the dipole MLWA contribution:

$$\sigma_{sca;E1} = \frac{4\pi}{15k^2} \frac{10x^6 |\varepsilon - 1|^2}{\left| \varepsilon + 2 - \frac{3}{5}(\varepsilon - 2)x^2 - i\frac{2}{3}(\varepsilon - 1)x^3 \right|^2}, \quad (15)$$

$$\sigma_{abs;E1} = \frac{4\pi}{15k^2} \frac{9x^3 (x^2 + 5) \Im(\varepsilon)}{\left| \varepsilon + 2 - \frac{3}{5}(\varepsilon - 2)x^2 - i\frac{2}{3}(\varepsilon - 1)x^3 \right|^2}, \quad (16)$$

$$\sigma_{ext;E1} = \frac{4\pi}{15k^2} \frac{9x^3 (x^2 + 5) \Im(\varepsilon) + 10x^6 |\varepsilon - 1|^2}{\left| \varepsilon + 2 - \frac{3}{5}(\varepsilon - 2)x^2 - i\frac{2}{3}(\varepsilon - 1)x^3 \right|^2}. \quad (17)$$

The unitarity of the MLWA, i.e. that  $\sigma_{ext;pl} = \sigma_{sca;pl} + \sigma_{abs;pl}$ , can be easily checked. One can also easily verify that, for  $\Im(\varepsilon) = 0$ , the common denominator  $|\Delta|^2$ ,  $\Delta(x) := F + D(x) - iR(x)$ , of the dipole MLWA cross sections (eqs 15–17) vanishes at

$$\Re(\varepsilon) \approx -2 - \frac{12x^2}{5} \quad (18)$$

up to the order  $x^2$ , in which case  $\Delta \approx \mathcal{O}(x^3)$ . The latter is, as it should, in agreement with the dipolar LSPR position in the exact Mie theory up to the order of  $x^2$  (see sec 12.1.1 of ref 11). The very same red-shift (eq 18) follows, as it should, also on using any of eqs 9–12. The easiest way to verify this is to substitute eq 18 into the respective denominators of eqs

9–12, whereby the real part of each denominator vanishes including the terms  $\mathcal{O}(x^2)$ . For a general  $(E\ell)$ -pole, the position of an  $(E\ell)$ -pole LSPR up to the order  $x^2$  can be implicitly found as

$$\Re(\varepsilon) \approx -\frac{\ell+1}{\ell} - \frac{2(\ell+1)(2\ell+1)}{\ell(2\ell-1)(2\ell+3)} x^2. \quad (19)$$

In order to better address the above intrinsic ambiguity of the MLWA, let us limit its definition as an approximation which satisfies the following axioms:

- (A1) It has the functional form (eq 6), with the Fröhlich term  $F$  and the radiative reaction term  $R$  fixed by eqs 7 and 13, respectively.
- (A2) A dynamic depolarization term  $D$  ( $\sim x^2$ ), required to be at most linear in  $\varepsilon$ , has to reproduce the red shift (eq 19).

The above axioms are obviously satisfied by the MLWA's (eq 10) and (eq 12). It is not difficult to demonstrate that for each  $\ell$  there is an infinite one parameter continuous family of MLWA's, which satisfy the above axioms **A1-A2**, yet they have all different dynamic depolarization term. Just assume  $D$  in the form

$$D = (\mathbf{a}\varepsilon + \mathbf{b})x^2, \quad \mathbf{b} = \frac{\ell+1}{\ell} \mathbf{a} + \frac{2(\ell+1)(2\ell+1)}{\ell(2\ell-1)(2\ell+3)}, \quad (20)$$

where  $\mathbf{a}, \mathbf{b}$  are real numbers. Note that

$$\begin{aligned} & \Im \left\{ (\varepsilon - 1) \left[ \varepsilon^* + \frac{\ell+1}{\ell} + (\mathbf{a}\varepsilon^* + \mathbf{b})x^2 \right] \right\} \\ &= \Im \left\{ \varepsilon \frac{\ell+1}{\ell} - \varepsilon^* + (-\mathbf{a}\varepsilon^* + \mathbf{b}\varepsilon)x^2 \right\} = \left[ \frac{(2\ell+1)}{\ell} + (\mathbf{a} + \mathbf{b})x^2 \right] \Im(\varepsilon), \end{aligned} \quad (21)$$

where we have used  $\Im(-\varepsilon^*) = \Im(\varepsilon)$  to arrive at the last equality. In the case of passive media without any gain  $\Im(\varepsilon) \geq 0$ . Thus the constraint 8 is automatically satisfied for  $\mathbf{a}, \mathbf{b} \geq 0$ . In particular, when eq 21 is combined with eq 20, eq 21 imposes a limitation

on  $x$  only for  $\mathbf{a} < 0$ , in which case the constraint becomes

$$1 + \left[ \mathbf{a} + \frac{2(\ell + 1)}{(2\ell - 1)(2\ell + 3)} \right] x^2 \geq 0.$$

In the limit  $\ell \gg 1$  this reduces to  $1 + \mathbf{a}x^2 \gtrsim 0$ , which is in agreement with that  $\mathbf{b} \approx \mathbf{a}$  for  $\ell \gg 1$ .

As it has been illustrated in Figure 1, altering the dynamic depolarization term  $D$ , while of course obeying the axiom **A2**, can have a very dramatic effect on the MLWA's predictions. In what follows, we exploit the untapped one-parameter freedom in selecting an optimized  $D$ .

## MLWA with Optimized Dynamic Depolarization Term

The results shown in Figure 2 demonstrate the effect of optimizing  $D$  on the contributions of  $\ell = 1, 2, 3$  electric multipoles to the extinction efficiency of Ag, Al, Au and Mg nanospheres using real material data. The noble metals Ag and Au are traditional plasmonic materials, yet they are rare and expensive. Al is much cheaper plasmonic metal, with resonances in the UV and visible up to  $\sim 700$  nm owing to a strong interband transition leading to high losses at lower energies.<sup>45,46</sup> Mg is one of the recently emerged plasmonic metals having a broad operating range. Recent experimental work has demonstrated that top-down fabricated Mg nanostructures sustain LSPRs.<sup>47,48</sup>

The results shown in Figures 3–6 provide a clear demonstration of that our  $\mathcal{O}(x^2)$  MLWA surprisingly yields very accurate results for plasmonic spheres both for (i)  $x$  up to  $\gtrsim 1$  and beyond, and (ii) higher order multipoles ( $\ell > 1$ ), essentially *doubling* its expected range of validity. The latter is, as shown in Figure 7, independent of a host. Quite unexpectedly, the precision of our results with an optimized  $D$  can be noticeably better than that involving the  $\mathcal{O}(x^4)$  approximation of ref 21, which is shown for a comparison in Figures 3–6. This observation becomes even more striking after analyzing  $\mathcal{O}(x^4)$  asymptotics ( $x \ll 1$ ) for

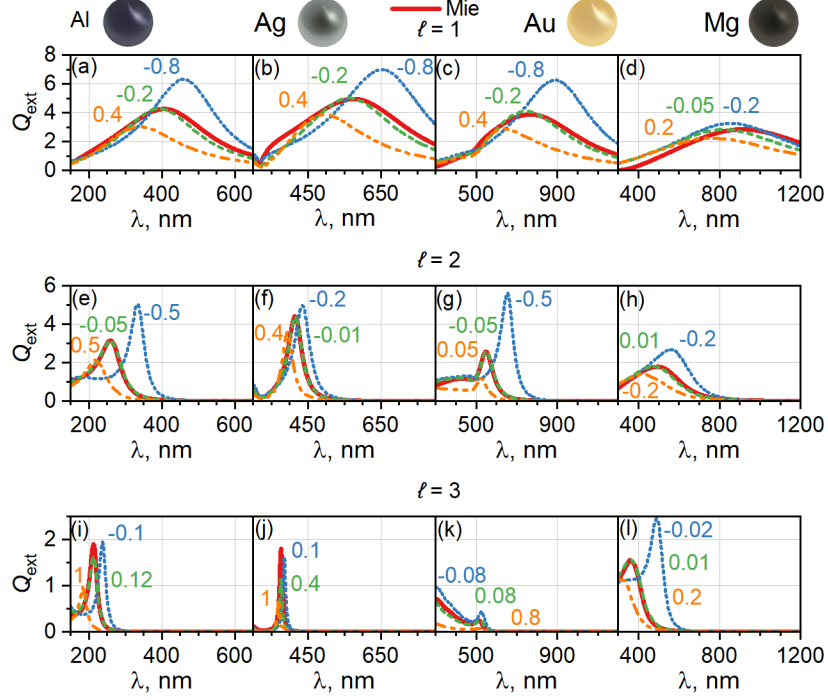


Figure 2: The effect of optimizing  $D$  on the contributions of  $\ell = 1, 2, 3$  electric multipoles to the extinction efficiency of Al, Ag, Au and Mg nanospheres with  $r_s = 50$  nm,  $r_s = 70$  nm,  $r_s = 100$  nm, and  $r_s = 120$  nm, respectively. Spectra are calculated via exact Mie theory (eq 4) and via MLWA (eq 6) with dynamic depolarization from eq 20 on using different  $\alpha$  as labeled in plots.

spherical Bessel functions and their fractions for arbitrary  $\ell$  (see Supporting Information) and realizing that its range of validity extends well beyond  $x = 1$  with deviations less than 1% with respect to exact results (Figures S1-S3, see the Supporting Information).

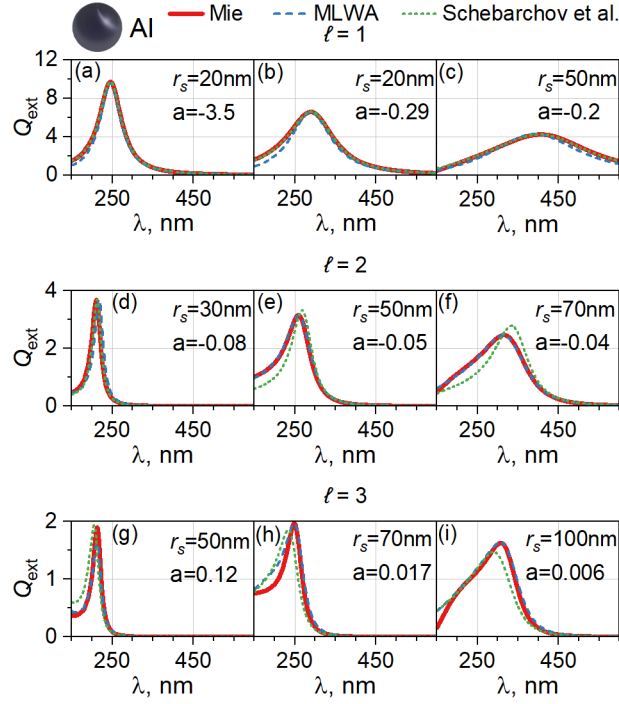


Figure 3: Comparison of the contributions of  $\ell = 1, 2, 3$  electric multipoles to the extinction efficiency of Al nanospheres in water ( $n_h = 1.33$ ) host as calculated via exact Mie theory (eq 4), via MLWA (eq 6) with dynamic depolarization from eq 20 on using optimized parameter  $\mathbf{a}$  as labeled in plots, and via eqs 32, 39 and 40 of ref 21 for  $\ell = 1, 2, 3$ , respectively. Notice different  $r_s$  are chosen for the most representative results.

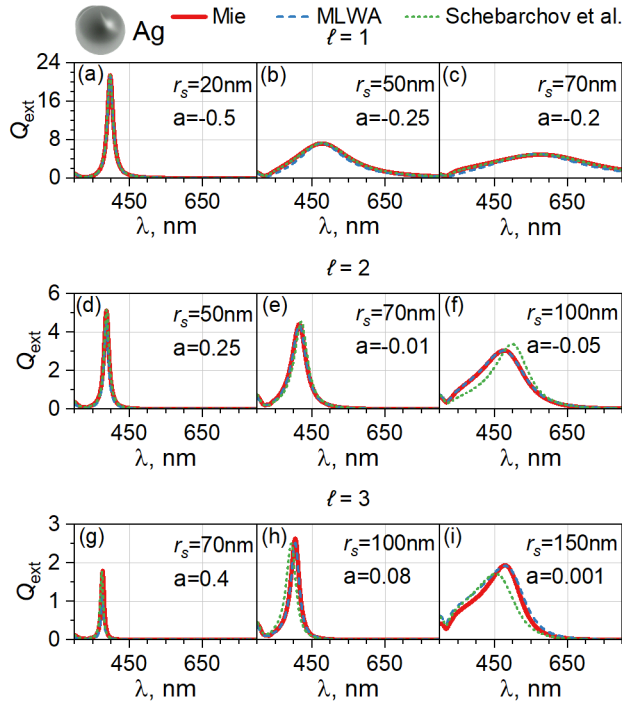


Figure 4: The same as in Figure 3, but for Ag spheres.

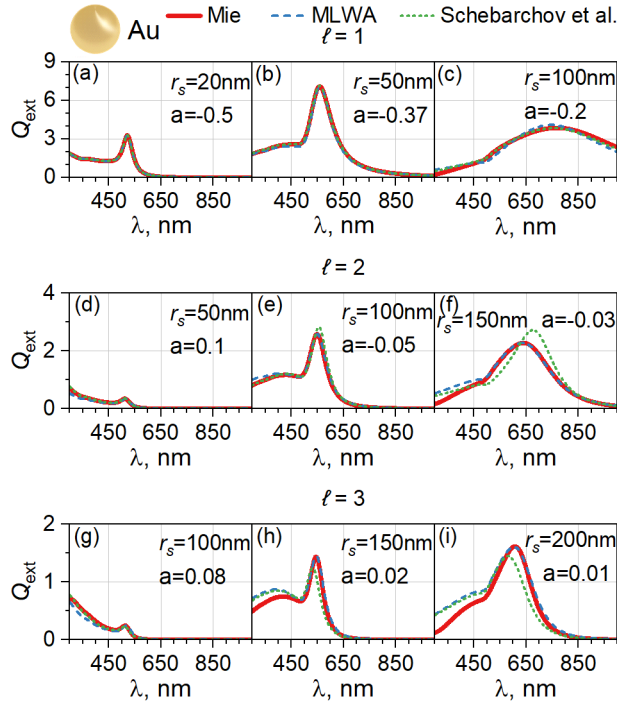


Figure 5: The same as in Figure 3, but for Au spheres.

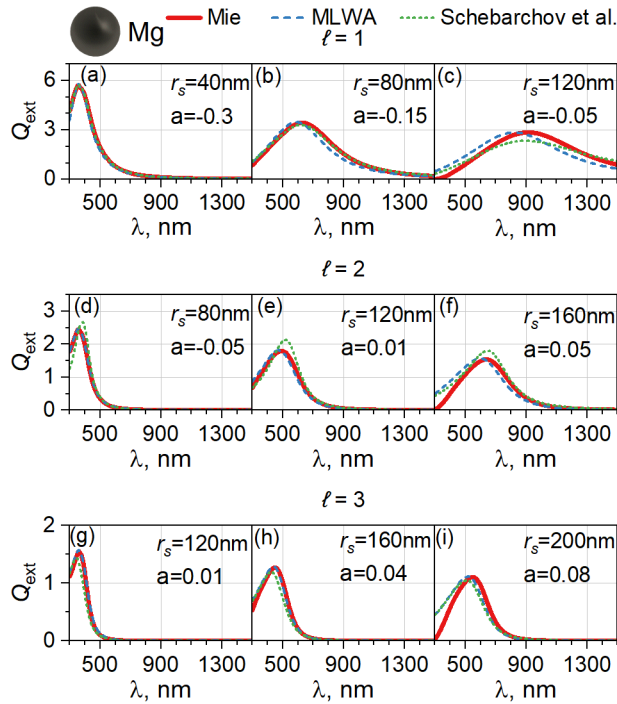


Figure 6: The same as in Figure 3, but for Mg spheres.

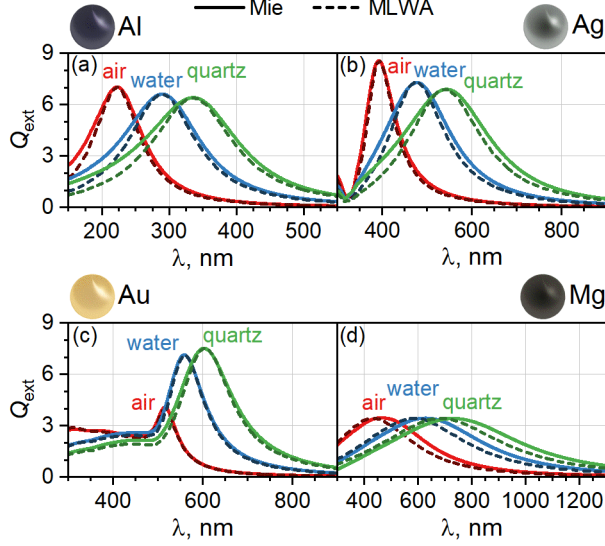


Figure 7: Electric dipole ( $\ell = 1$ ) contribution to the extinction efficiency of Al, Ag, Au, and Mg nanospheres with  $r_s = 30$  nm,  $r_s = 50$  nm,  $r_s = 50$  nm, and  $r_s = 80$  nm, respectively, embedded in air ( $n_h = 1.00$ ), water ( $n_h = 1.33$ ) and quartz ( $n_h = 1.50$ ) medium. Spectra are calculated via exact Mie theory (eq 4) shown in full line, and via MLWA (eq 6) shown by dashed line, with dynamic depolarization from eq 20 using optimized values of parameter  $\alpha$  (for air, water, and quartz, respectively): (a)  $-0.29$ ,  $-0.29$ ,  $-0.29$ ; (b)  $-0.3$ ,  $-0.25$ ,  $-0.23$ ; (c)  $-0.41$ ,  $-0.37$ ,  $-0.33$ ; (d)  $-0.11$ ,  $-0.13$ ,  $-0.14$ .

## Discussion and Open Questions

There is a number of novel features in our approach. For instance, an ambiguity of the MLWA has been spotted earlier,<sup>17,21</sup> yet the infinite one parameter continuous family of MLWA's has not been noted before. Some partial extension of the MLWA for  $\ell = 2, 3$  has been presented by Schebarchov et al.,<sup>21</sup> however no general formulas valid for any  $\ell$  have been presented. Other points are discussed below.

### Comparison of $\mathcal{O}(x^2)$ and $\mathcal{O}(x^4)$ Approximations

The MLWA form of  $T_{E1}$  (eq 14) as discussed in ref 17 (see eq A3 therein) has been improved with a quartic  $\sim x^4$  term in its denominator (eq 33 of ref 21), and its domain of validity has been investigated (Figure 3 of ref 21), together with its generalization for  $\ell = 2, 3$  (Figure 4 of ref 21). A distinct advantage of the  $\mathcal{O}(x^4)$  approximation of Schebarchov et al.<sup>21</sup> is



that one has a fixed formula for all particle parameters. However, the  $\mathcal{O}(x^4)$  approximation disguises that our  $\mathcal{O}(x^2)$  MLWA with an optimized dynamic depolarization term  $D$  can actually improve on the predictive power of the  $\mathcal{O}(x^4)$  approximation. The very fact that by dropping  $\mathcal{O}(x^4)$  terms and keeping only terms  $\mathcal{O}(x^2)$ , while optimizing  $D$ , one can improve precision, as highlighted in Figures 3–7, is not only surprising but also bears important physical consequences. Indeed, in a bottom-up approach to depolarization,<sup>17</sup> the absence of any  $\mathcal{O}(x^4)$  term and the sole presence of only  $\mathcal{O}(x^2)$  term in depolarization is a consequence of assuming the internal field  $\mathbf{E}_{in}$  within the particle to be *uniform* and *constant* on the application of a constant applied field  $\mathbf{E}_0$ . The latter is rigorously true in electrostatics for a particle with a general ellipsoid shape. With an increasing particle size, this is less and less true and deviations from the uniformity of  $\mathbf{E}_{in}$  begins to grow up. The fact that  $\mathcal{O}(x^2)$  MLWA remains still very good approximation signifies that it is possible to describe the particle properties with a kind of a uniform effective internal field  $\bar{\mathbf{E}}_{in}$ . The fitting parameter  $\mathbf{a}$  of  $D$  in eq 20 might have then an interpretation as a weighting parameter enabling to relate  $\bar{\mathbf{E}}_{in} = \int_V \mathbf{E}_{in} d^3\mathbf{r}$ , where the integration is over a particle volume, to an applied field  $\mathbf{E}_0$  with a constant amplitude. (Note in passing that for  $x \gtrsim 1$  we can no longer assume  $\mathbf{E}_0$  to be constant over particle volume.) Because the profile of  $\mathbf{E}_{in}$  is expected to change with particle radius  $r_s$ , the latter could explain why a given radius subinterval requires its own  $\mathbf{a}$  for the best fit. A dependence of  $\mathbf{a}$  on  $r_s$  should not be confused with a size  $x$ -dependence, because  $\mathbf{a}$  does *not* depend on the wavelength  $\lambda$  (cf. Figures 3–7).

Last but not the least, recent work by Januar et al.<sup>22</sup> has shown that the  $\mathcal{O}(x^2)$  MLWA description of a Drude-like plasmonic particle translates straightforwardly into an equivalent intuitive description of scattering and near-field properties in terms of a driven damped harmonic oscillator with the Abraham-Lorentz force, mass, and stiffness all directly related to corresponding partial depolarization terms.<sup>22</sup> Our work thus extends the validity of the intuitive driven damped harmonic oscillator description to much larger particle sizes, whereby significantly improved understanding of nanoparticle scattering and near-field properties can

be achieved.

## MLWA and Padé Approximation

The MLWA form (eq 6) with the size-independent quasi-static Fröhlich term (eq 7), a dynamic depolarization term  $D$  (eq 20), and the radiative reaction term  $R_{E\ell}$  (eq 13) is in its essence a rational polynomial approximation to the exact T-matrix for each given  $\ell$ . In order to address an intrinsic ambiguity of  $D$  term in a “fixed formula for all particle parameters” approach, a useful criterion could be how a particular  $\ell$ th channel MLWA compares against the so-called  $[(2\ell + 1)/(2\ell + 1)]_{T_{p\ell}}(x)$  Padé approximation<sup>49,50</sup> of the exact T-matrix  $T_{p\ell}$ . For this purpose one has to compare the first  $4\ell + 2$  derivatives at  $x = 0$  of the MLWA ( $M$  in eqs SI.21, see Supporting Information) against those of the rigorous  $\ell$ -channel  $T$ -matrix ( $f$  in eqs SI.21, see Supporting Information). In this regard note that any change of  $D$  induces changes in the Taylor expansion of a  $\ell$ th channel MLWA in any order  $\sim x^{2\ell+1+2k}$ ,  $k \geq 1$ . If the respective derivatives do agree, then the MLWA can be seen as the Padé approximation of the T-matrix. One can compute the first  $4\ell + 2$  derivatives for the functional MLWA form 6 (see Supplementary Information). Alas, the computation of the first  $4\ell + 2$  derivatives at  $x = 0$  of the exact  $\ell$ -channel  $T$ -matrix seems to be too involved.

## Summary and Conclusions

An intermediate range of sizes ( $r_s \gtrsim 20$  nm) of nanoparticles clearly shows inadequacy of the Rayleigh limit in their description. The lack of unitarity and size dependency, together with further shortcomings, of the latter, can be easily overcome by the MLWA, which provides an economic and concise description of photonic properties of nanoparticles in any multipole order  $\ell$  in terms of a size-independent quasi-static Fröhlich term  $F$  (eq 7), a dynamic depolarization term  $D$  (eq 20), and a radiative reaction term  $R$  ( $\sim x^{2\ell+1}$ ) (eq 13), all combined together in the functional form (eq 6). On making use of that there is an *infinite* one pa-

parameter set of different MLWA's which all satisfy the axioms **A1-A2**, we have determined for each multipole order  $\ell$  an optimal dynamic depolarization term, which yields the best agreement with the Mie theory. Surprisingly enough, such an optimized MLWA has been shown to provide a very reliable description even for particle size parameter  $x \gtrsim 1$ , essentially doubling its expected range of validity, which is much larger than has been ever expected to be possible. Our results can be used in a number of different directions and settings:

- Numerical methods such as CDA and DDA<sup>29-31</sup> divide scatterer into a large discrete set of subunits and provide a means for calculating its optical response as the result of interaction of elementary dipoles, each of which corresponding to one of the scatterer subunits, and each described by its own dipole polarizability. Since particle dipole polarizability  $\alpha_1$  is directly related to the dipole  $T_{E1}$  by  $\alpha_1 = -3iT_{E1}/(2k^3)$ , any method which is intrinsically based on elementary polarizabilities, can, in principle, benefit by adopting our results.
- Using dipole MLWA polarizabilities, one can obtain an intermediary Maxwell-Garnett formula improving the usual quasi-static Maxwell-Garnett formula, while providing an insight into the extended Maxwell-Garnett formula.<sup>26,51</sup>
- In addition to the dipole MLWA as in ref 33, the higher-order MLWA results of this paper can be straightforwardly used to further amend the Gersten and Nitzan (GN) quasi-static approximation for determining nonradiative decay rates<sup>32</sup> by making use of more precise particle multipolar polarizabilities. Our results could hopefully lead to improving the GN approximation, which at present works for core-shell particles much worse<sup>52</sup> than for homogeneous particles.<sup>33</sup>
- Our precise approximation of  $T_{E\ell}$  can be employed also for a deeper understanding of plasmonic sensing,<sup>53-55</sup> colors,<sup>56</sup> and other applications<sup>57</sup> as an interplay of three elementary terms  $F$ ,  $D$ , and  $R$ .

- An intuitive description of the dipole contribution of Drude-like plasmonic particles in terms of a driven damped harmonic oscillator<sup>22</sup> may offer deeper insight into the above applications. Keeping only  $\mathcal{O}(x^2)$  terms has a distinct advantage: higher-order ( $\ell > 1$ ) MLWA of Drude-like plasmonic particles could, in principle, be intuitively described in terms of a driven damped harmonic oscillator with a higher-order Abraham-Lorentz force, mass, and stiffness directly related to corresponding depolarization terms, thereby extending validity of the results of ref 22 to much larger particle sizes than initially expected. There is a hope that such an intuitive description could, in addition to a red-shift of near-field maximum,<sup>58</sup> enable to describe also a blue-shift of absorption maximum.<sup>23</sup>
- Our MLWA expression can be straightforwardly implemented within traditional multiple-scattering theories<sup>34-38</sup> to analyze in simple terms the effect of periodic arrangement of spherical scatterers in a plane, or in a three-dimensional lattice, on various single-sphere multipole contributions.
- Our finding of the one-parameter freedom of the dynamic depolarization term could be of use also for other particle shapes and compositions. For example, the applicability of the MLWA extends to spheroids,<sup>16,17,22</sup> which yield for suitable aspect ratios remarkably good approximation for disks (for instance, disks with height 20 nm and radii from 20 to 250 nm were approximated as oblate spheroids in ref 18), rods,<sup>54</sup> cubes and cuboids,<sup>19</sup> core-shell,<sup>21,59</sup> multilayered,<sup>60</sup> and graded-index particles.<sup>61</sup>

Such an economic description of plasmonic properties as an interplay of three elementary terms  $F$ ,  $D$ , and  $R$ , provided by the MLWA, is easy to analyze and understand, and thus design nanoparticles with desired properties at the expense of using inherently sophisticated and difficult to understand spherical Bessel and Hankel functions. Hopefully in the future no review on plasmonic properties of small metal particles will ever ignore the MLWA.<sup>42</sup>

## Supporting Information Available

$\mathcal{O}(x^4)$  expansion of spherical Bessel functions and their fractions for arbitrary  $\ell$ ; MLWA derivations; MLWA and driven damped harmonic oscillator model; Padé approximation.

## References

1. Mie, G. Beiträge zur Optik trüber Medien, speziell kolloidaler Metallösungen. *Annalen der Physik* **1908**, *330*, 377–445.
2. Hamam, R. E.; Karalis, A.; Joannopoulos, J. D.; Soljačić, M. Coupled-mode theory for general free-space resonant scattering of waves. *Physical Review A* **2007**, *75*, 053801.
3. Ruan, Z.; Fan, S. Temporal coupled-mode theory for Fano resonance in light scattering by a single obstacle. *Journal of Physical Chemistry C* **2010**, *114*, 7324–7329.
4. Ruan, Z.; Fan, S. Design of subwavelength superscattering nanospheres. *Applied Physics Letters* **2011**, *98*, 043101.
5. Joe, Y. S.; Satanin, A. M.; Kim, C. S. Classical analogy of Fano resonances. *Physica Scripta* **2006**, *74*, 259–266.
6. Gallinet, B.; Martin, O. J. F. Influence of electromagnetic interactions on the line shape of plasmonic Fano resonances. *ACS Nano* **2011**, *5*, 8999–9008.
7. Limonov, M. F.; Rybin, M. V.; Poddubny, A. N.; Kivshar, Y. S. Fano resonances in photonics. *Nature Photonics* **2017**, *11*, 543–554.
8. Grigoriev, V.; Tahri, A.; Varault, S.; Rolly, B.; Stout, B.; Wenger, J.; Bonod, N. Optimization of resonant effects in nanostructures via Weierstrass factorization. *Physical Review A* **2013**, *88*, 011803.

9. Colom, R.; Devilez, A.; Enoch, S.; Stout, B.; Bonod, N. Polarizability expressions for predicting resonances in plasmonic and Mie scatterers. *Physical Review A* **2017**, *95*, 063833.
10. Colom, R.; McPhedran, R.; Stout, B.; Bonod, N. Modal analysis of anapoles, internal fields, and Fano resonances in dielectric particles. *Journal of the Optical Society of America B* **2019**, *36*, 2052–2061.
11. Bohren, C. F.; Huffman, D. R. *Absorption and scattering of light by small particles*; Wiley-VCH Verlag GmbH: Weinheim, Germany, 1998; p 530.
12. Moskovits, M. Surface-enhanced spectroscopy. *Reviews of Modern Physics* **1985**, *57*, 783–826.
13. Meier, M.; Wokaun, A. Enhanced fields on large metal particles: dynamic depolarization. *Optics Letters* **1983**, *8*, 581–583.
14. Zeman, E. J.; Schatz, G. C. An accurate electromagnetic theory study of surface enhancement factors for silver, gold, copper, lithium, sodium, aluminum, gallium, indium, zinc, and cadmium. *Journal of Physical Chemistry* **1987**, *91*, 634–643.
15. Kelly, K. L.; Coronado, E.; Zhao, L. L.; Schatz, G. C. The optical properties of metal nanoparticles: The influence of size, shape, and dielectric environment. *Journal of Physical Chemistry B* **2003**, *107*, 668–677.
16. Kuwata, H.; Tamaru, H.; Esumi, K.; Miyano, K. Resonant light scattering from metal nanoparticles: Practical analysis beyond Rayleigh approximation. *Applied Physics Letters* **2003**, *83*, 4625–4627.
17. Moroz, A. Depolarization field of spheroidal particles. *Journal of the Optical Society of America B* **2009**, *26*, 517–527.

18. Zorić, I.; Zäch, M.; Kasemo, B.; Langhammer, C. Gold, platinum, and aluminum nanodisk plasmons: Material independence, subradiance, and damping mechanisms. *ACS Nano* **2011**, *5*, 2535–2546.
19. Massa, E.; Maier, S. A.; Giannini, V. An analytical approach to light scattering from small cubic and rectangular cuboidal nanoantennas. *New Journal of Physics* **2013**, *15*, 063013.
20. Le Ru, E. C.; Somerville, W. R. C.; Auguie, B. Radiative correction in approximate treatments of electromagnetic scattering by point and body scatterers. *Physical Review A* **2013**, *87*, 012504.
21. Schebarchov, D.; Auguie, B.; Le Ru, E. C. Simple accurate approximations for the optical properties of metallic nanospheres and nanoshells. *Physical Chemistry Chemical Physics* **2013**, *15*, 4233–4242.
22. Januar, M.; Liu, B.; Cheng, J.-C.; Hatanaka, K.; Misawa, H.; Hsiao, H.-H.; Liu, K.-C. Role of depolarization factors in the evolution of a dipolar plasmonic spectral line in the far- and near-field regimes. *Journal of Physical Chemistry C* **2020**, *124*, 3250–3259.
23. Rasskazov, I. L.; Carney, P. S.; Moroz, A. Intriguing branching of the maximum position of the absorption cross section in Mie theory explained. *Optics Letters* **2020**, *45*, 4056–4059.
24. McPeak, K. M.; Jayanti, S. V.; Kress, S. J. P.; Meyer, S.; Iotti, S.; Rossinelli, A.; Norris, D. J. Plasmonic films can easily be better: Rules and recipes. *ACS Photonics* **2015**, *2*, 326–333.
25. Palm, K. J.; Murray, J. B.; Narayan, T. C.; Munday, J. N. Dynamic optical properties of metal hydrides. *ACS Photonics* **2018**, *5*, 4677–4686.

26. Yannopapas, V.; Moroz, A. Negative refractive index metamaterials from inherently non-magnetic materials for deep infrared to terahertz frequency ranges. *Journal of Physics: Condensed Matter* **2005**, *17*, 3717–3734.
27. Markel, V. A. Introduction to the Maxwell Garnett approximation: tutorial. *Journal of the Optical Society of America A* **2016**, *33*, 1244.
28. Markel, V. A. Maxwell Garnett approximation (advanced topics): tutorial. *Journal of the Optical Society of America A* **2016**, *33*, 2237.
29. Purcell, E. M.; Pennypacker, C. R. Scattering and absorption of light by nonspherical dielectric grains. *The Astrophysical Journal* **1973**, *186*, 705–714.
30. Draine, B. T.; Flatau, P. J. Discrete-dipole approximation for scattering calculations. *Journal of the Optical Society of America A* **1994**, *11*, 1491–1499.
31. Yurkin, M.; Hoekstra, A. The discrete dipole approximation: An overview and recent developments. *Journal of Quantitative Spectroscopy and Radiative Transfer* **2007**, *106*, 558–589.
32. Gersten, J.; Nitzan, A. Spectroscopic properties of molecules interacting with small dielectric particles. *Journal of Chemical Physics* **1981**, *75*, 1139–1152.
33. Moroz, A. Non-radiative decay of a dipole emitter close to a metallic nanoparticle: Importance of higher-order multipole contributions. *Optics Communications* **2010**, *283*, 2277–2287.
34. Korringa, J. On the calculation of the energy of a Bloch wave in a metal. *Physica* **1947**, *13*, 392–400.
35. Kohn, W.; Rostoker, N. Solution of the Schrödinger equation in periodic lattices with an application to metallic lithium. *Physical Review* **1954**, *94*, 1111–1120.



36. Moroz, A. Density-of-states calculations and multiple-scattering theory for photons. *Physical Review B* **1995**, *51*, 2068–2081.
37. Moroz, A.; Sommers, C. Photonic band gaps of three-dimensional face-centred cubic lattices. *J. Phys.: Condens. Mat.* **1999**, *11*, 997–1008.
38. Stefanou, N.; Yannopapas, V.; Modinos, A. Heterostructures of photonic crystals: frequency bands and transmission coefficients. *Computer Physics Communications* **1998**, *113*, 49–77.
39. Newton, R. G. *Scattering Theory of Waves and Particles*; Springer, Berlin, Heidelberg, 1982; p 745.
40. Abramowitz, M.; Stegun, I. A. *Handbook of Mathematical Functions*; Dover Publications: New York, 1973; p 1046.
41. Chýlek, P.; Pinnick, R. G. Nonunitarity of the light scattering approximations. *Applied Optics* **1979**, *18*, 1123–1124.
42. Fan, X.; Zheng, W.; Singh, D. J. Light scattering and surface plasmons on small spherical particles. *Light: Science & Applications* **2014**, *3*, e179.
43. Yezekyan, T.; Nerkararyan, K. V.; Bozhevolnyi, S. I. Maximizing absorption and scattering by spherical nanoparticles. *Optics Letters* **2020**, *45*, 1531–1534.
44. Olver, F. W.; Lozier, D. W.; Boisvert, R. F.; Clark, C. W. *NIST Handbook of Mathematical Functions*, 1st ed.; Cambridge University Press, 2010.
45. Langhammer, C.; Schwind, M.; Kasemo, B.; Zorić, I. Localized surface plasmon resonances in aluminum nanodisks. *Nano Letters* **2008**, *8*, 1461–1471.
46. Ross, M. B.; Schatz, G. C. Aluminum and indium plasmonic nanoantennas in the ultraviolet. *Journal of Physical Chemistry C* **2014**, *118*, 12506–12514.

47. Biggins, J. S.; Yazdi, S.; Ringe, E. Magnesium nanoparticle plasmonics. *Nano Letters* **2018**, *18*, 3752–3758.
48. Ringe, E. Shapes, plasmonic properties, and reactivity of magnesium nanoparticles. *Journal of Physical Chemistry C* **2020**, *124*, 15665–15679.
49. Baker, G. A.; Graves-Morris, P. *Padé Approximants*; Encyclopedia of Mathematics and its Applications; Cambridge University Press, 2010.
50. Press, W. H.; Teukolsky, S. A.; Vetterling, W. T.; Flannery, B. P. *Numerical Recipes: The Art of Scientific Computing*, 3rd ed.; Cambridge University Press, 2007.
51. Ruppin, R. Evaluation of extended Maxwell-Garnett theories. *Optics Communications* **2000**, *182*, 273–279.
52. Sun, S.; Rasskazov, I. L.; Carney, P. S.; Zhang, T.; Moroz, A. Critical role of shell in enhanced fluorescence of metal-dielectric core-shell nanoparticles. *Journal of Physical Chemistry C* **2020**, *124*, 13365–13373.
53. Otte, M. A.; Sepúlveda, B.; Ni, W.; Juste, J. P.; Liz-Marzán, L. M.; Lechuga, L. M. Identification of the optimal spectral region for plasmonic and nanoplasmonic sensing. *ACS Nano* **2010**, *4*, 349–357.
54. Jakab, A.; Rosman, C.; Khalavka, Y.; Becker, J.; Trügler, A.; Hohenester, U.; Sönnichsen, C. Highly sensitive plasmonic silver nanorods. *ACS Nano* **2011**, *5*, 6880–6885.
55. Reed, J. C.; Zhu, H.; Zhu, A. Y.; Li, C.; Cubukcu, E. Graphene-enabled silver nanoantenna sensors. *Nano Letters* **2012**, *12*, 4090–4094.
56. Wen, L.; Chen, Q.; Hu, X.; Wang, H.; Jin, L.; Su, Q. Multifunctional silicon optoelectronics integrated with plasmonic scattering color. *ACS Nano* **2016**, *10*, 11076–11086.

57. Pirzadeh, Z.; Pakizeh, T.; Miljkovic, V.; Langhammer, C.; Dmitriev, A. Plasmon-interband coupling in nickel nanoantennas. *ACS Photonics* **2014**, *1*, 158–162.
58. Zuloaga, J.; Nordlander, P. On the energy shift between near-field and far-field peak intensities in localized plasmon systems. *Nano Letters* **2011**, *11*, 1280–1283.
59. Chung, H. Y.; Leung, P. T.; Tsai, D. P. Dynamic modifications of polarizability for large metallic spheroidal nanoshells. *Journal of Chemical Physics* **2009**, *131*, 124122.
60. Chung, H. Y.; Guo, G. Y.; Chiang, H.-P.; Tsai, D. P.; Leung, P. T. Accurate description of the optical response of a multilayered spherical system in the long wavelength approximation. *Physical Review B* **2010**, *82*, 165440.
61. Chung, H. Y.; Leung, P. T.; Tsai, D. P. Modified long wavelength approximation for the optical response of a graded-index plasmonic nanoparticle. *Plasmonics* **2012**, *7*, 13–18.

# Supporting Information:

## Remarkable Predictive Power of the Modified Long Wavelength Approximation

Ilia L. Rasskazov,<sup>†</sup> Vadim I. Zakomirnyi,<sup>\*,‡,¶</sup> Anton D. Utyushev,<sup>‡,¶</sup> P. Scott  
Carney,<sup>†</sup> and Alexander Moroz<sup>\*,§</sup>

<sup>†</sup>*The Institute of Optics, University of Rochester, Rochester, NY 14627, USA*

<sup>‡</sup>*Siberian Federal University, Krasnoyarsk, 660041, Russia*

<sup>¶</sup>*Institute of Computational Modelling of the Siberian Branch of the Russian Academy of  
Sciences, Krasnoyarsk, 660036, Russia*

<sup>§</sup>*Wave-scattering.com*

E-mail: vadimza@icm.krasn.ru; wavescattering@yahoo.com

### $\mathcal{O}(x^4)$ Expansion of Spherical Bessel Functions and Their Fractions for Arbitrary $\ell$

The results of this section allows us to generalize the order  $\mathcal{O}(x^4)$  approximation of Schebar-  
chov et al.<sup>S1</sup> for  $\ell > 3$ . In doing so, we shall generalize Lewin's function and its asymptotic<sup>S2</sup>  
for an arbitrary  $\ell$ .

Asymptotic expansion of the familiar spherical Bessel functions  $j_\ell$  and  $n_\ell$  for  $z \rightarrow 0$

involving the first three orders is:<sup>S3</sup>

$$\begin{aligned}
(10.1.2) : j_\ell(z) &\sim \frac{z^\ell}{(2\ell+1)!!} \left[ 1 - \frac{z^2}{2(2\ell+3)} + \frac{z^4}{8(2\ell+3)(2\ell+5)} \right], \\
[zj_\ell(z)]' &\sim \frac{z^\ell}{(2\ell+1)!!} \left[ (\ell+1) - \frac{z^2}{2} \frac{\ell+3}{2\ell+3} + \frac{z^4}{8} \frac{\ell+5}{(2\ell+3)(2\ell+5)} \right], \\
(10.1.3) : n_\ell(z) &\sim -\frac{(2\ell-1)!!}{z^{\ell+1}} \left[ 1 + \frac{z^2}{2(2\ell-1)} + \frac{z^4}{8(2\ell-3)(2\ell-1)} \right], \\
[zn_\ell(z)]' &\sim \frac{(2\ell-1)!!}{z^{\ell+1}} \left[ \ell + \frac{z^2}{2} \frac{\ell-2}{2\ell-1} + \frac{z^4}{8} \frac{\ell-4}{(2\ell-3)(2\ell-1)} \right], \tag{SI.1}
\end{aligned}$$

where the number in parenthesis on the left corresponds to the formula of ref S3. Note in passing that although one can use  $[zf_\ell(z)]' = zf_{\ell-1}(z) - \ell f_\ell(z)$ , which is the recurrence (10.1.21) of ref S3, to determine  $[zf_\ell(z)]'$  for a given spherical Bessel function  $f_\ell$ , it is much easier to perform instead direct differentiation of the asymptotic series. Using eq (SI.1), one finds

$$\begin{aligned}
\frac{j_\ell(z)}{[zj_\ell(z)]'} &\sim \frac{1}{(\ell+1)} \left[ 1 + \frac{z^2}{(\ell+1)(2\ell+3)} \right], \\
\frac{n_\ell(z)}{[zn_\ell(z)]'} &\sim -\frac{1}{\ell} \left[ 1 + \frac{z^2}{\ell(2\ell-1)} \right]. \tag{SI.2}
\end{aligned}$$

In order to determine  $\mathcal{O}(x^4)$  correction, one has to expand

$$\begin{aligned}
\frac{1}{[zj_\ell(z)]'} &\sim \frac{(2\ell+1)!!}{(\ell+1)z^\ell} \left[ 1 - \frac{(\ell+3)z^2}{2(\ell+1)(2\ell+3)} + \frac{(\ell+5)z^4}{8(\ell+1)(2\ell+3)(2\ell+5)} \right]^{-1} \\
&\sim \frac{(2\ell+1)!!}{(\ell+1)z^\ell} (1-A)^{-1} \\
&\sim \frac{(2\ell+1)!!}{(\ell+1)z^\ell} (1+A+A^2), \tag{SI.3}
\end{aligned}$$

and collect in each of  $A$  and  $A^2$  the terms up to  $\mathcal{O}(z^4)$ . The latter means keeping whole

$$A := \frac{(\ell+3)z^2}{2(\ell+1)(2\ell+3)} - \frac{(\ell+5)z^4}{8(\ell+1)(2\ell+3)(2\ell+5)}, \tag{SI.4}$$

whereas, in the case of  $A^2$ , keeping in eq (SI.3) only the term

$$A^2 \sim \frac{(\ell + 3)^2 z^4}{4(\ell + 1)^2 (2\ell + 3)^2}.$$

The  $\mathcal{O}(z^4)$ -term of the ratio in eq (SI.3) is thus

$$\mathcal{O}(z^4) = \frac{\ell[\ell(2\ell + 19) + 68] + 75}{8(\ell + 1)^2 (2\ell + 3)^2 (2\ell + 5)} z^4.$$

Using the above results, it is straightforward to determine the asymptotic of the Bessel functions fractions

$$\begin{aligned} F_\ell(z) &:= \frac{(\ell + 1)j_\ell(z)}{[zj_\ell(z)]'} = \frac{(\ell + 1)j_\ell(z)}{zj_{\ell-1}(z) - \ell j_\ell(z)}, \\ G_\ell(z) &:= -\frac{\ell n_\ell(z)}{[zn_\ell(z)]'} = \frac{\ell n_\ell(z)}{\ell n_\ell(z) - zn_{\ell-1}(z)}. \end{aligned} \tag{SI.5}$$

In arriving at the second equalities in (SI.5), the recurrence (cf eq 10.1.21 of S3)

$$[zf_\ell(z)]' = zf_{\ell-1}(z) - \ell f_\ell(z)$$

satisfied by the spherical Bessel functions has been used.

The  $\mathcal{O}(z^4)$ -term of the ratio in the first formula in (SI.2) is formally obtained by making use of the formula

$$(1 + Az^2 + Bz^4)(1 + Cz^2 + Dz^4) \sim 1 + (A + C)z^2 + (B + D + AC)z^4 + \dots,$$

where the first factor is  $j_\ell$  expansion in the 2nd line of eqs (SI.1), and the second factor is the resulting  $\mathcal{O}(z^4)$  expansion in eq (SI.3). In the formula here,  $A$  is no longer given by a temporary label in eq (SI.4) but rather  $\mathcal{O}(z^2)$ -term of the expansion of  $j_\ell$  in the 2nd line of

eqs (SI.1). The ultimate  $\mathcal{O}(z^4)$  term reads as

$$\mathcal{O}(z^4) = \frac{3(2 + \ell)z^4}{(5 + 2\ell)(3 + 5\ell + 2\ell^2)^2}.$$

Thus, combining everything together,

$$F_\ell(z) \sim 1 + \frac{z^2}{(\ell + 1)(2\ell + 3)} + \frac{3(\ell + 2)}{2\ell + 5} \left[ \frac{z^2}{(\ell + 1)(2\ell + 3)} \right]^2. \quad (\text{SI.6})$$

One can verify that, for  $\ell = 1$ , the familiar asymptotic of Lewin's function  $F_1$  is recovered,

$$F_1(z) \sim 1 + \frac{z^2}{10} + \frac{9z^4}{700}. \quad (\text{SI.7})$$

Similarly, repeating all the above steps for the second equation in eq (SI.2), we get:

$$G_\ell(z) \sim 1 + \frac{z^2}{\ell(2\ell - 1)} + \frac{3(\ell - 1)}{2\ell - 3} \left[ \frac{z^2}{\ell(2\ell - 1)} \right]^2. \quad (\text{SI.8})$$

Fig S1 is crucial for understanding both the range of validity of the MLWA and why the  $\mathcal{O}(x^2)$  approximation can, in principle, be at least as good as the  $\mathcal{O}(x^4)$  approximation. One sees that both approximations, in the case of either  $F_\ell$  or  $G_\ell$ , essentially overlies with the corresponding exact expression of  $F_\ell$  or  $G_\ell$  on the real axis. For instance, each of the  $\mathcal{O}(x^2)$  and the  $\mathcal{O}(x^4)$  approximations (SI.7) deviates from the exact values of  $F_1(z)$  for *real*  $x$  with not more than 1% for  $x$  up to  $x \approx 1.34$ . The respective  $\mathcal{O}(x^2)$  and  $\mathcal{O}(x^4)$  approximations begin to significantly deviate with the corresponding exact expression of  $F_\ell$  or  $G_\ell$  at nearly the same point of the real axis.

It has been known that, for purely *real* values of  $x$  in the dipole case,  $F_1(x)$  is monotonically increasing with increasing  $x$  up to the first pole of  $F_1(x)$  at  $x = 2.74370725179062$ . We see analogous behaviour also for  $\ell > 1$ , with the pole position shifting to larger  $x$  with increasing  $\ell$ .

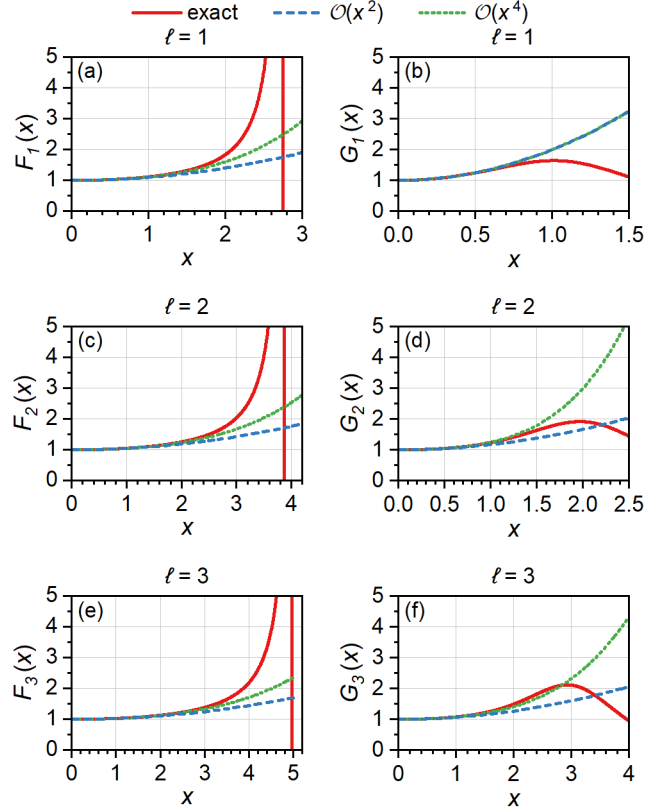


Figure S1: A graphical illustration of the range of validity of the respective  $\mathcal{O}(x^2)$  and  $\mathcal{O}(x^4)$  asymptotic expansions of  $F_\ell$  and  $G_\ell$  showing that they can be approximated on the real axis with the accuracy higher than 1% for  $\ell \leq 3$ . Note is passing that  $F_\ell$  can be approximated on a larger interval of the real axis well beyond  $x \gtrsim 1$  than corresponding  $G_\ell$ . However, any attempt to approximate  $F_\ell$  on a real interval any further eventually breaks down due to the first pole of  $F_\ell$ .

Table S1: Values of  $x_{max}$  for which  $\mathcal{O}(x^2)$  and  $\mathcal{O}(x^4)$  approximations of  $F_\ell(x)$  and  $G_\ell(x)$  given in eqs (SI.6) and (SI.8) are valid with up to 1% accuracy for  $0 < x < x_{max}$  (cf. Figure S1)

$F_\ell(x)$			$G_\ell(x)$		
$\ell$	$\mathcal{O}(x^2)$	$\mathcal{O}(x^4)$	$\ell$	$\mathcal{O}(x^2)$	$\mathcal{O}(x^4)$
1	0.92	1.34	1	0.57	0.57
2	1.34	1.89	2	0.61	0.99
3	1.74	2.46	3	0.99	1.34



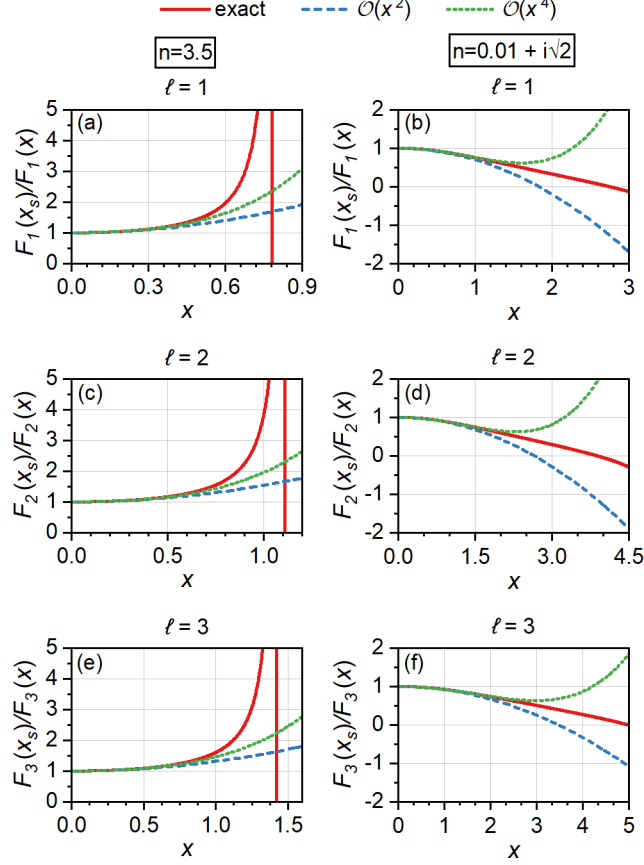


Figure S2: A graphical illustration of the range of validity of the respective  $\mathcal{O}(x^2)$  and  $\mathcal{O}(x^4)$  asymptotic expansions of  $F_\ell(x_s)/F_\ell(x)$  for real (left) and complex (right) relative refractive index contrast,  $n = n_s/n_h$ . The right panels here corresponds to  $\varepsilon = n^2 \approx -2$ , i.e. to a proximity of the dipole LSPR. Similarly to Figure S1,  $\mathcal{O}(x^2)$  and  $\mathcal{O}(x^4)$  approximations essentially overlies with the corresponding exact expression for a long stretch of  $x$  on the real axis.

On following similar steps as above, one obtains the following asymptotic of the ratios

$$\begin{aligned}
F_\ell(x_s)/F_\ell(x) &\sim 1 + \frac{(n^2 - 1)x^2}{(\ell + 1)(2\ell + 3)} \\
&+ \left[ \frac{3(\ell + 2)(n^4 - 1) - (2\ell + 5)n^2}{2\ell + 5} + \frac{1}{(\ell + 1)^2(2\ell + 3)^2} \right] \left[ \frac{x^2}{(\ell + 1)(2\ell + 3)} \right]^2, \\
F_\ell(x_s)/G_\ell(x) &\sim 1 + \left[ \frac{n^2}{(\ell + 1)(2\ell + 3)} - \frac{1}{\ell(2\ell - 1)} \right] x^2 \\
&+ \left[ \frac{3(\ell + 2)n^4}{(2\ell + 5)(\ell + 1)^2(2\ell + 3)^2} - \frac{n^2}{\ell(\ell + 1)(2\ell - 1)(2\ell + 3)} - \frac{1}{\ell(2\ell - 3)(2\ell - 1)^2} \right] x^4.
\end{aligned} \tag{SI.9}$$

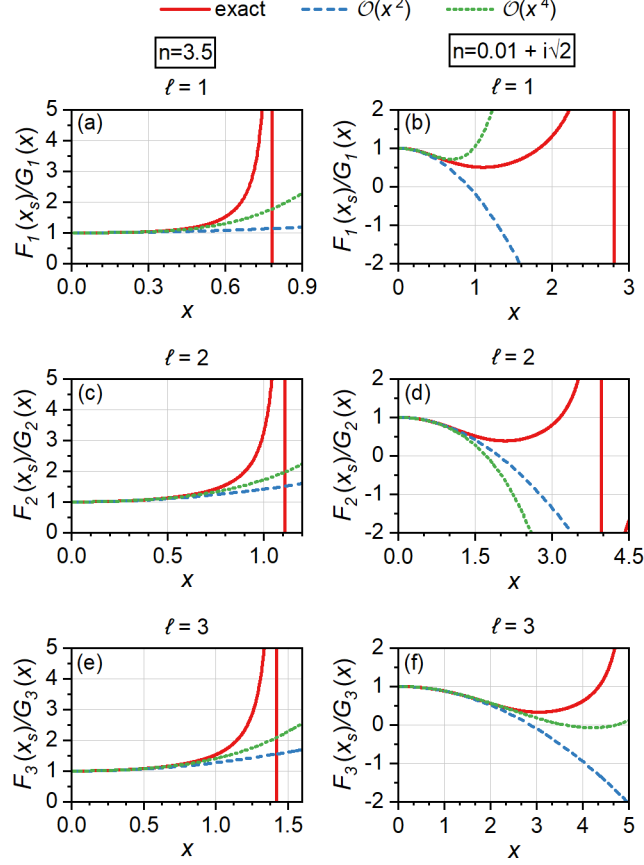


Figure S3: The same as in Figure S2, but for  $F_\ell(x_s)/G_\ell(x)$ . Crucially, and much the same in Fig. S2, the respective  $\mathcal{O}(x^2)$  and  $\mathcal{O}(x^4)$  approximations overlies in a proximity of the dipole LSPR for  $\varepsilon = n^2 \approx -2$ , as shown in the right panels, over longer  $x$  interval with the exact expressions. This is the reason why MLWA works better for plasmonic particles than for purely dielectric particles.

The above ratios play a very significant role in determining the so-called *renormalized* dielectric permittivity and magnetic permeability as in eq (SI.10) below.

The precision of the above asymptotic formulas, and their range of applicability, strongly depend on how  $x_s$  moves in the complex plane of  $x_s$  with varying  $\lambda$ . As seen in Table S2 and Figures S2 and S3, the real axis provides the largest restriction on the use of above asymptotic formulas. Contrary to that, in a Drude-like regime, the complex refractive index  $n = n_r + i\kappa$ ,  $\kappa \geq 0$  is necessarily dominated in magnitude by its imaginary part  $\kappa$ . The latter is obvious from that  $n^2 = n_r^2 - \kappa^2 + 2in_r\kappa$  has to reproduce the Drude dielectric function characterized by a negative real part, which magnitude can be appreciable. Therefore, for

Table S2: Values of  $x_{max}$  for which  $\mathcal{O}(x^2)$  and  $\mathcal{O}(x^4)$  approximations of  $F_\ell(x_s)/F_\ell(x)$  and  $G_\ell(x_s)/F_\ell(x)$  given in eqs (SI.9) are valid with up to 1% accuracy for  $0 < x < x_{max}$  (cf. Figures S2 and S3). The complex value of  $n$  corresponds to  $\varepsilon = n^2 \approx -2$ , i.e. to a proximity of the dipole LSPR.

$n = 3.5$						$n = 0.01 + i\sqrt{2}$					
$F_\ell(x_s)/F_\ell(x)$			$F_\ell(x_s)/G_\ell(x)$			$F_\ell(x_s)/F_\ell(x)$			$F_\ell(x_s)/G_\ell(x)$		
$\ell$	$\mathcal{O}(x^2)$	$\mathcal{O}(x^4)$	$\ell$	$\mathcal{O}(x^2)$	$\mathcal{O}(x^4)$	$\ell$	$\mathcal{O}(x^2)$	$\mathcal{O}(x^4)$	$\ell$	$\mathcal{O}(x^2)$	$\mathcal{O}(x^4)$
1	0.27	0.38	1	0.27	0.40	1	0.62	1.06	1	0.30	0.46
2	0.39	0.55	2	0.42	0.56	2	0.89	1.51	2	1.08	0.80
3	0.50	0.71	3	0.52	0.72	3	1.16	1.95	3	1.43	1.47

metal particles,  $x_s$  moves in the complex plane of  $x_s$  closer to the positive imaginary axis than to the real axis, as is the case of purely dielectric particles. The latter is the main reason of a much larger range validity of the MLWA for plasmonic particles compared to dielectric ones, as demonstrated in Table S2 and Figures S2 and S3.

## MLWA Derivations

In this section, we derive a general form of transfer-matrix  $T_{E\ell}$  in the MLWA limit and arrive to eqs 9–12. In doing so we also generalize the order  $\mathcal{O}(x^4)$  approximation of Schebarchov et al.<sup>S1</sup> for an arbitrary  $\ell$ . The asymptotic expansions are used in accordance with our rules **(R1)**-**(R2)**. In order to make it unambiguous, we will be expanding spherical Bessel functions in each of the numerator and denominator of the fraction of eq 4 defining the  $T$ -matrix, and *not* expanding the fraction of eq 4 into the Taylor series at  $x = 0$ .

Scattering can be equally well described by any of the three familiar inter-related  $T$ ,  $S$ , and  $K$  matrices:

$$T = \frac{1}{2}(S - 1), \quad S = 1 + 2T, \quad K = \frac{iT}{1 + T} = -i\frac{1 - S}{1 + S}, \quad S = \frac{1 - iK}{1 + iK},$$

where the  $S$  matrix is related by the Cayley transform with the inverse  $K^{-1}$  of the  $K$  matrix. This is not surprising, because the Cayley transform  $f(z) = (z - i)/(z + i)$  maps the real

line to the unit circle, and the unitarity of the  $S$  matrix amounts to reality of the  $K$  matrix. In terms of a scattering phase shift  $\eta$ , one has  $S = e^{2i\eta}$ ,  $T = i \sin \eta e^{i\eta}$ , and  $K = -\tan \eta$ .

In the present 3D problem of electromagnetic scattering from a sphere,

$$\begin{aligned} K_{p\ell} &= -\frac{j_\ell(x)[x_s j_\ell(x_s)]' - v j_\ell(x_s)[x j_\ell(x)]'}{n_\ell(x)[x_s j_\ell(x_s)]' - v j_\ell(x_s)[x n_\ell(x)]'} \\ &= \frac{v j_\ell(x_s)[x j_\ell(x)]' - j_\ell(x)[x_s j_\ell(x_s)]'}{-v j_\ell(x_s)[x n_\ell(x)]' + n_\ell(x)[x_s j_\ell(x_s)]'} \\ &= \frac{j_\ell(x)}{n_\ell(x)} \frac{v F_\ell(x_s)/F_\ell(x) - 1}{v[F_\ell(x_s)/G_\ell(x)][\ell/(\ell+1)] + 1}, \end{aligned}$$

where  $v = \mu_s/\mu_h$  for  $p = M$ , and  $v = \varepsilon_s/\varepsilon_h$  for  $p = E$ ,  $j_\ell$ ,  $n_\ell$  are the usual spherical Bessel functions (see Sec. 10 of ref S3), and the shorthands  $F_\ell$  and  $G_\ell(x)$  have been introduced by eq (SI.5). Let

$$\tilde{v}_\ell = v F_\ell(x_s)/F_\ell(x), \quad \hat{v}_\ell = v F_\ell(x_s)/G_\ell(x). \quad (\text{SI.10})$$

Then

$$K_{p\ell} = \frac{j_\ell(x)}{n_\ell(x)} \frac{\tilde{v} - 1}{\ell \hat{v}/(\ell+1) + 1}. \quad (\text{SI.11})$$

The function  $F_\ell(x_s)$  has been for  $\ell = 1$  introduced by Lewin<sup>S2</sup> and employed by e.g. Sarychev, McPhedran, and Shalaev<sup>S4</sup> and many others<sup>S5</sup> to define, as in the last two equations above, the so-called *renormalized* dielectric permittivity and magnetic permeability.

The advantage of making use of the  $K$  matrix is that it is *real* in purely dielectric case and enables one to write the  $T$  matrix as

$$T_{p\ell} = \frac{-i K_{p\ell}}{1 + i K_{p\ell}}. \quad (\text{SI.12})$$

Now, the first fraction on the rhs of eq (SI.11) reduces for  $x \ll 1$  to a numerical prefactor  $-(\ell+1)x^{2\ell+1}/(2\ell-1)!(2\ell+1)!!$  (see formulas 10.53.1-2 in ref S6), which enables one to

introduce a renormalized polarization factor

$$Q_{p\ell} = -\frac{(2\ell-1)!!(2\ell+1)!!}{(\ell+1)x^{2\ell+1}} K_{p\ell} \rightarrow \frac{\tilde{v}_\ell - 1}{\ell\hat{v}_\ell + (\ell+1)} \quad (x \ll 1).$$

Correspondingly,  $T_{p\ell}$  in eq (SI.12) can be recast as

$$\begin{aligned} T_{p\ell} &= i \frac{(\ell+1)x^{2\ell+1}}{(2\ell-1)!!(2\ell+1)!!} Q_{p\ell} \left( 1 - i \frac{(\ell+1)x^{2\ell+1}}{(2\ell-1)!!(2\ell+1)!!} Q_{p\ell} \right)^{-1} \\ &= i \frac{(\ell+1)x^{2\ell+1}}{\ell(2\ell-1)!!(2\ell+1)!!} (\tilde{v}_\ell - 1) \left( \frac{\ell+1}{\ell} + \hat{v}_\ell - i \frac{(\ell+1)x^{2\ell+1}}{\ell(2\ell-1)!!(2\ell+1)!!} (\tilde{v}_\ell - 1) \right)^{-1}. \end{aligned} \quad (\text{SI.13})$$

The equation is starting point at arriving at general  $\ell$ -pole MLWA, eqs 9–12. The latter requires to consider intermediate values of  $x$ , which necessitates to keep  $\mathcal{O}(x^2)$  terms in the asymptotic of the ratios in eqs (SI.9), or

$$\begin{aligned} F_\ell(x_s)/F_\ell(x) &\sim 1 + \frac{(n^2-1)x^2}{(\ell+1)(2\ell+3)}, \\ F_\ell(x_s)/G_\ell(x) &\sim 1 + \left( \frac{n^2}{(\ell+1)(2\ell+3)} - \frac{1}{\ell(2\ell-1)} \right) x^2. \end{aligned} \quad (\text{SI.14})$$

For  $p = E$  polarization, one arrives on combining (SI.13) and (SI.14) at the MLWA limit

$$T_{E\ell} \sim \frac{iR(x)}{\varepsilon + \frac{\ell+1}{\ell} + \frac{\varepsilon}{(\ell+1)(2\ell+3)} \left( n^2 - \frac{(\ell+1)(2\ell+3)}{\ell(2\ell-1)} \right) x^2 - iR(x)}, \quad (\text{SI.15})$$

where

$$R(x) = \frac{(\ell+1)x^{2\ell+1}}{\ell(2\ell-1)!!(2\ell+1)!!} \left[ \varepsilon - 1 + \frac{(n^2-1)\varepsilon x^2}{(\ell+1)(2\ell+3)} \right].$$

On substituting  $n^2 = \varepsilon$  one arrives at our expression 9. The *dynamic depolarization* term  $D$  ( $\sim x^2$ ) originates on expanding  $x$ -dependent  $\hat{v}_\ell$  in (SI.13). Obviously, one finds the usual

quasi-static limit for  $p = E$  upon neglecting the  $\mathcal{O}(x^2)$  terms in eq (SI.15), or when

$$Q_{E\ell} \rightarrow \frac{(\varepsilon_s/\varepsilon_h) - 1}{\ell(\varepsilon_s/\varepsilon_h) + (\ell + 1)} = \frac{1}{\ell} \frac{(\varepsilon_s/\varepsilon_h) - 1}{\frac{\ell+1}{\ell} + (\varepsilon_s/\varepsilon_h)}.$$

is substituted into first equality in eq (SI.13).

Note in passing that the form of the limit expression (SI.15) is ambiguous and, by multiplying both the numerator and denominator of (SI.15) by  $1 - \varepsilon x^2/[(\ell + 1)(2\ell + 3)]$ , it can be reduced to our expression 10,

$$T_{E\ell} \sim \frac{iR_{E\ell}}{\varepsilon + \frac{\ell+1}{\ell} - \frac{2(2\ell+1)}{\ell(2\ell-1)(2\ell+3)} \varepsilon x^2 - iR_{E\ell}}.$$

Upon using the asymptotic expansions (Ch. 10 of ref S6), while following our recipe **(R1)** of keeping only terms up to  $\mathcal{O}(x^2)$  in the asymptotic expansion of each spherical Bessel function, and that

$$\frac{d}{dr}[rf(kr)] = \frac{d}{d(kr)}[krf(kr)],$$

the denominator in the expression 4 of the  $T$ -matrix is given by

$$i[vv'_\ell(k_2r_s)u_\ell(k_1r_s) - v_\ell(k_2r_s)u'_\ell(k_1r_s)] = ir_s \frac{(2\ell - 1)!!}{(2\ell + 1)!!} \frac{x_s^\ell}{x^{\ell+1}} \times \left[ v \left( \ell + \frac{x^2}{2} \frac{\ell - 2}{2\ell - 1} - \frac{x_s^2}{2} \frac{\ell}{2\ell + 3} \right) + \ell + 1 + \frac{x^2}{2} \frac{\ell + 1}{2\ell - 1} - \frac{x_s^2}{2} \frac{\ell + 3}{2\ell + 3} \right],$$

where  $u_\ell(x) = xj_\ell(x)$  and  $v_\ell(x) = xn_\ell(x)$  are the usual Riccati-Bessel functions (see Sec. 10.3 S3). Upon taking into account that  $x_s^2 = x^2 n_s^2/n_h^2$ , one finds eventually for the denominator of the  $T$ -matrix

$$i[vv'_\ell(k_2r_s)u_\ell(k_1r_s) - v_\ell(k_2r_s)u'_\ell(k_1r_s)] = ir_s \frac{(2\ell - 1)!!}{(2\ell + 1)!!} \frac{x_s^\ell}{x^{\ell+1}} \times \left\{ \ell v + (\ell + 1) + \frac{x^2}{2(2\ell + 3)} \left[ -\ell v^2 - \frac{3(2\ell + 1)}{(2\ell - 1)} v + \frac{(\ell + 1)(2\ell + 3)}{2\ell - 1} \right] + \mathcal{O}(x^4) \right\}. \quad (\text{SI.16})$$

The numerator in the expression 4 of the  $T$ -matrix is given by

$$\begin{aligned}
& [vu'_\ell(k_2r_s)u_\ell(k_1r_s) - u_\ell(k_2r_s)u'_\ell(k_1r_s)] = r_s[vu'_\ell(k_2r_s)j_\ell(k_1r_s) - j_\ell(k_2r_s)u'_\ell(k_1r_s)] = \\
& r_s \frac{x_s^\ell x^\ell}{[(2\ell+1)!!]^2} \times \\
& \left\{ v \left[ (\ell+1) - \frac{x^2}{2} \frac{\ell+3}{2\ell+3} \right] \left( 1 - \frac{x_s^2}{2(2\ell+3)} \right) - \left( 1 - \frac{x^2}{2(2\ell+3)} \right) \left[ (\ell+1) - \frac{x_s^2}{2} \frac{\ell+3}{2\ell+3} \right] \right\} \\
& = r_s \frac{x_s^\ell x^\ell}{[(2\ell+1)!!]^2} (\ell+1)(v-1) \left\{ 1 - (v+1) \frac{x^2}{2(2\ell+3)} + \mathcal{O}(x^4) \right\}. \tag{SI.17}
\end{aligned}$$

Hence, upon combining the numerator asymptotic  $N$  given by (SI.17), and the denominator asymptotic  $D$  given by (SI.16), one finds our MLWA expression 11,

$$\begin{aligned}
T_{E\ell} &= -\frac{N}{N+D} \sim -\frac{N}{D} \\
&\sim \frac{i\ell R_{E\ell} \left[ 1 - (\varepsilon+1) \frac{x^2}{2(2\ell+3)} \right]}{\ell\varepsilon + \ell + 1 + \frac{x^2}{2(2\ell+3)} \left[ -\ell\varepsilon^2 - \frac{3(2\ell+1)}{2\ell-1} \varepsilon + \frac{(\ell+1)(2\ell+3)}{2\ell-1} \right] - i\ell R_{E\ell}}. \tag{SI.18}
\end{aligned}$$

As it has been alluded to in connection with the limit expression (SI.15), the limit form (SI.18) of  $T_{E\ell}$  is ambiguous and can, by multiplying both the numerator and denominator by  $1 + (\varepsilon+1)x^2/[2(2\ell+3)]$ , be alternatively recast as

$$T_{E\ell} \sim \frac{iR_{E\ell}}{\varepsilon + \frac{\ell+1}{\ell} + [(\ell-2)\varepsilon + \ell + 1] \frac{(2\ell+1)x^2}{\ell(2\ell-1)(2\ell+3)} - iR_{E\ell}},$$

which is the MLWA with  $D(x)$  of eq 12.

On substituting full formulas (SI.9) into eq (SI.10) determining the renormalized dielectric permittivity and magnetic permeability, one immediately obtains an extension of the  $\mathcal{O}(x^4)$  approximation of Schebarchov et al.<sup>S1</sup> for an arbitrary  $\ell$ . In this case, our rules **(R1)**-**(R2)** are obviously amended to include also the terms  $\mathcal{O}(x^4)$  in the corresponding asymptotic expansions of Bessel functions.

# MLWA and Driven Damped Harmonic Oscillator Model

In this section, we provide guidelines for using our MLWA (eq 6), with the size-independent quasi-static Fröhlich term (eq 7), a dynamic depolarization term  $D$  (eq 20), and the radiative reaction term  $R_{E\ell}$  (eq 13) in harmonic oscillator model.<sup>S7</sup>

A free electron of mass  $m_e$  and charge  $-e$  in an external harmonic field  $\mathbf{E}_0$  obeys a simple equation for a driven damped harmonic oscillator,

$$m_e \ddot{\mathbf{X}} + m_e \gamma \dot{\mathbf{X}} = -e \mathbf{E}_0. \quad (\text{SI.19})$$

Here  $\mathbf{X}$  denotes the harmonic displacement of the electron ( $\mathbf{X}(\omega) = \mathbf{X}_0 e^{-i\omega t}$ ) and an overdot stands for time derivative. Equation (SI.19) is a starting point at arriving at the Drude formula for bulk electrons.<sup>S8,S9</sup> The Drude loss term,  $\gamma$ , is similar to *viscous damping*, indicating damping that is proportional to the collision rate of electrons, also known as intraband transition damping.

However, within a particle the incoming electric field  $\mathbf{E}_0$  is modified due to the induced depolarization field to  $\mathbf{E}_{in} := \mathbf{E}_0 + \mathbf{E}_d$ , where the induced depolarization field,

$$\mathbf{E}_d = -\frac{1}{\varepsilon_h} \mathbf{L}_{eff} \cdot \mathbf{P},$$

takes into account the change of external harmonic field  $\mathbf{E}_0$  as felt by electrons inside the particle. The field is directly proportional to the effective depolarization factor  $\mathbf{L}_{eff}$  and the polarization  $\mathbf{P}$ .

For our MLWA one finds in the dipole case

$$L_{eff}(x) = L - \frac{\mathbf{a}\varepsilon + \mathbf{b}}{3(\varepsilon - 1)} x^2 - i\frac{2}{9} x^3,$$

with  $L$  being the well-known *geometrical factor* (cf. eq 5.32 of ref S10), which accounts for the shape of a particle. In particular,  $L = 1/3$  for a sphere. The dipole polarizability can be



recast as

$$\alpha_{MWLA} = \frac{V}{4\pi} \frac{\varepsilon - 1}{1 + L_{eff}(x)(\varepsilon - 1)}.$$

To comply with ref S7, we recast  $L_{eff}(x)$  as  $L_{eff}(\omega)$  on making use of that dimensionless  $x = kr_s = (\omega/c)n_h r_s$ ,

$$L_{eff}(\omega) = L - \frac{\mathbf{a}\varepsilon + \mathbf{b}}{3(\varepsilon - 1)c^2} \omega^2 - i \frac{2}{9c^3} \omega^3 = L - L_d \omega^2 - i L_{rad} \omega^3. \quad (\text{SI.20})$$

On using the equation above instead of eqs 9 and 13 of ref S7, the range of validity of results presented in ref S7 can, in principle, be extended to larger particles, even though  $L_{eff}(\omega)$  in eq (SI.20) is  $\varepsilon$ -dependent.

## Padé Approximation

Given a function  $f$  and two integers  $s \geq 0$  and  $t \geq 1$ , the Padé approximant of order  $[s/t]$  is the rational function

$$M(x) = \frac{\sum_{j=0}^s a_j x^j}{1 + \sum_{k=1}^t b_k x^k} = \frac{a_0 + a_1 x + a_2 x^2 + \cdots + a_s x^s}{1 + b_1 x + b_2 x^2 + \cdots + b_t x^t},$$

which agrees with  $f(x)$  to the highest possible order  $x^{s+t}$ , which amounts to

$$\begin{aligned} f(0) &= M(0), \\ f'(0) &= M'(0), \\ f''(0) &= M''(0), \\ &\vdots \\ f^{(s+t)}(0) &= M^{(s+t)}(0). \end{aligned} \quad (\text{SI.21})$$

The Padé approximant defined above is also denoted as  $[s/t]_f(x)$ .

Now consider an explicit form of the MLWA of eq 20,

$$T_{p\ell} \sim \frac{iR_{E\ell}(x)}{v + \frac{\ell+1}{\ell} + (\mathbf{a}\varepsilon + \mathbf{b})x^2 - iR_{E\ell}(x)}.$$

It is tempting to compare the  $\ell$ th channel MLWA against the so-called  $[(2\ell + 1)/(2\ell + 1)]_{T_\ell}(x)$  rational Padé approximation of the corresponding exact  $\ell$ th channel  $T$ -matrix  $T_{E\ell}$ . In doing so, one has to demonstrate that our MLWA ( $M$  in eqs (SI.21)) has identical first  $4\ell + 2$  derivatives at  $x = 0$  as the rigorous  $\ell$ -channel  $T$ -matrix ( $f$  in eqs (SI.21)). If such a comparison can have been established, this would have explained

- (1) why a particular MLWA is singled out from all possible MLWA approximations in the  $x \ll 1$  range
- (2) its success for  $x \gtrsim 1$  (a kind of resummation) (Note in passing that any fraction leads to infinite Taylor series in  $x$ .)

On introducing a shorthand  $\Delta(x) := F + D(x) - iR(x)$  in eq 6, together with the respective shorthands  $d_\ell$  and  $r_\ell$  for  $x$ -independent factors in  $D(x)$  and  $R(x)$ , one can verify that the only nonzero derivatives of  $\Delta$ ,  $D(x)$  and  $R(x)$  in the limit  $x \rightarrow 0$  are

$$\begin{aligned} D^{(2)}(0) &= 2d_\ell, & R^{(2\ell+1)}(0) &= (2\ell + 1)! r_\ell, \\ \Delta(0) &= F, & \Delta^{(2)}(0) &= D^{(2)}(0) = 2d_\ell, \\ \Delta^{(2\ell+1)}(0) &= -iR^{(2\ell+1)}(0) = -i(2\ell + 1)! r_\ell. \end{aligned} \tag{SI.22}$$

In virtue of the general *Leibniz rule*, one finds for the  $n$ th derivative of  $T_{E\ell}(x)$  of eq 6

$$T_{E\ell}^{(n)}(0) = i \sum_{k=0}^n \binom{n}{k} R^{(k)}(0) [\Delta^{-1}(0)]^{(n-k)},$$

where  $\binom{n}{k}$  is the familiar binomial coefficient. In virtue of (SI.22)

$$\begin{aligned} T_{E\ell}^{(n)}(0) &\equiv 0, \quad n = 0, 1, \dots, 2\ell, \\ T_{E\ell}^{(2\ell+1)}(0) &= iR^{(2\ell+1)}(0)\Delta^{-1}(0) = \frac{i(2\ell+1)!r_\ell}{F}, \end{aligned}$$

whereas for  $n > 2\ell + 1$

$$T_{E\ell}^{(n)}(0) = i \binom{n}{2\ell+1} R^{(2\ell+1)}(0) [\Delta^{-1}(0)]^{(n-1-2\ell)} = i \binom{n}{2\ell+1} (2\ell+1)! r_\ell [\Delta^{-1}(0)]^{(n-1-2\ell)}. \quad (\text{SI.23})$$

In order to determine  $[\Delta^{-1}(0)]^{(k)}$ , one can make use of the Faà di Bruno's formula<sup>S11</sup>

$$\frac{d^n}{dx^n} f(g(x)) = \sum \frac{n!}{m_1! m_2! \dots m_n!} \cdot f^{(m_1+\dots+m_n)}(g(x)) \times \prod_{j=1}^n \left( \frac{g^{(j)}(x)}{j!} \right)^{m_j}, \quad (\text{SI.24})$$

where the sum is over all  $n$ -tuples of nonnegative integers  $(m_1, \dots, m_n)$  satisfying the constraint  $1 \cdot m_1 + 2 \cdot m_2 + 3 \cdot m_3 + \dots + n \cdot m_n = \sum_{j=1}^n j m_j = n$  (obviously some of  $m_j$ 's will be zero).

The point of crucial importance is that, in virtue of (SI.22), the rhs of (SI.24) is, in the case of  $g = \Delta$ , *nonzero* only for  $j = 2$  and  $m_2 = n/2$ , i.e. requiring  $n$  to be an *even* number and all other  $m_j \equiv 0$ ,  $j \neq 2$ ,  $n < 2\ell + 1$ . Therefore for  $n < 2\ell + 1$  one finds

$$\begin{aligned} [\Delta^{-1}(x)]^{(n)} &= \frac{n!}{(n/2)!} (-1)^{n/2} (n/2)! \Delta^{-(n/2)-1}(x) \left( \frac{\Delta^{(2)}(x)}{2!} \right)^{n/2} \\ &\rightarrow (-1)^{n/2} n! F^{-(n/2)-1} d_\ell^{n/2} \quad (x \rightarrow 0) \end{aligned}$$

On substituting the result back into (SI.23), where  $[\Delta^{-1}(0)]^{(n-1-2\ell)}$ , one finds for  $2\ell + 1 < n \leq 4\ell + 1$  (i.e.  $0 \leq n - 1 - 2\ell < 2\ell + 1$ ) and  $n$  *odd*

$$\begin{aligned} T_{E\ell}^{(n)}(0) &= i(-1)^{(n-1-2\ell)/2} \binom{n}{2\ell+1} (n-1-2\ell)! (2\ell+1)! r_\ell F^{-((n-1-2\ell)/2)-1} d_\ell^{(n-1-2\ell)/2} \\ &= i(-1)^{(n-1-2\ell)/2} n! r_\ell F^{-((n-1-2\ell)/2)-1} d_\ell^{(n-1-2\ell)/2}, \end{aligned}$$

whereas  $T_{E\ell}^{(n)}(0) \equiv 0$  for  $n$  even.

Eventually, given that

$$[\Delta^{-1}(0)]^{(2\ell+1)} = i(2\ell+1)!F^{-2}r_\ell \quad (x \rightarrow 0),$$

one finds for even  $n = 2(2\ell+1)$

$$\begin{aligned} T_{E\ell}^{(4\ell+2)}(0) &= i \binom{4\ell+2}{2\ell+1} (2\ell+1)! r_\ell [\Delta^{-1}(0)]^{(2\ell+1)} \\ &= - \binom{4\ell+2}{2\ell+1} F^{-2} [(2\ell+1)! r_\ell]^2 \\ &= -(4\ell+2)! F^{-2} r_\ell^2. \end{aligned}$$

**Important:** When comparing with the derivatives  $T_{E\ell}^{(n)}(0)$  in the exact Mie theory, one has to consider the variable  $x_s = n_s x$  as dependent on  $x$ .

## References

- (S1) Schebarchov, D.; Augu  , B.; Le Ru, E. C. Simple accurate approximations for the optical properties of metallic nanospheres and nanoshells. *Physical Chemistry Chemical Physics* **2013**, *15*, 4233–4242.
- (S2) Lewin, L. The electrical constants of a material loaded with spherical particles. *Journal of the Institution of Electrical Engineers-Part III: Radio and Communication Engineering* **1947**, *94*, 65–68.
- (S3) Abramowitz, M.; Stegun, I. A. *Handbook of Mathematical Functions*; Dover Publications: New York, 1973; p 1046.
- (S4) (a) Sarychev, A. K.; McPhedran, R. C.; Shalaev, V. M. Electrodynamics of metal-dielectric composites and electromagnetic crystals. *Physical Review B* **2000**, *62*, 8531–

- 8539; (b) Sarychev, A. K.; McPhedran, R. C.; Shalaev, V. M. Erratum: Electrodynamics of metal-dielectric composites and electromagnetic crystals [Phys. Rev. B 62 , 8531 (2000)]. *Physical Review B* **2001**, *64*, 079904.
- (S5) Yannopapas, V.; Moroz, A. Negative refractive index metamaterials from inherently non-magnetic materials for deep infrared to terahertz frequency ranges. *Journal of Physics: Condensed Matter* **2005**, *17*, 3717–3734.
- (S6) Olver, F. W.; Lozier, D. W.; Boisvert, R. F.; Clark, C. W. *NIST Handbook of Mathematical Functions*, 1st ed.; Cambridge University Press, 2010.
- (S7) Januar, M.; Liu, B.; Cheng, J.-C.; Hatanaka, K.; Misawa, H.; Hsiao, H.-H.; Liu, K.-C. Role of depolarization factors in the evolution of a dipolar plasmonic spectral line in the far- and near-field regimes. *Journal of Physical Chemistry C* **2020**, *124*, 3250–3259.
- (S8) Kittel, C. *Introduction to Solid State Physics*, 8th ed.; Wiley, 2004; p 704.
- (S9) Jackson, J. D. *Classical electrodynamics*, 3rd ed.; John Wiley & Sons, Inc., 1999; p 808.
- (S10) Bohren, C. F.; Huffman, D. R. *Absorption and scattering of light by small particles*; Wiley-VCH Verlag GmbH: Weinheim, Germany, 1998; p 530.
- (S11) (a) Di Bruno, F. F. Sullo sviluppo delle funzioni. *Annali di scienze matematiche e fisiche* **1855**, *6*, 479–480; (b) Di Bruno, F. F. Note sur une nouvelle formule de calcul différentiel. *Quarterly J. Pure Appl. Math* **1857**, *1*, 12.